Live cell imaging to understand monocyte, macrophage, and dendritic cell function in atherosclerosis

Sara McArdle, Zbigniew Mikulski, and Klaus Ley

Division of Inflammation Biology and Microscopy Core, La Jolla Institute of Allergy and Immunology, La Jolla, CA 92037

Intravital imaging is an invaluable tool for understanding the function of cells in healthy and diseased tissues. It provides a window into dynamic processes that cannot be studied by other techniques. This review will cover the benefits and limitations of various techniques for labeling and imaging myeloid cells, with a special focus on imaging cells in atherosclerotic arteries. Although intravital imaging is a powerful tool for understanding cell function, it alone does not provide a complete picture of the cell. Other techniques, such as flow cytometry and transcriptomics, must be combined with intravital imaging to fully understand a cell's phenotype, lineage, and function.

Intravital imaging has been used to visualize diverse leukocyte behaviors in a variety of contexts. Cell motion (Germain et al., 2012), cell proliferation (Stoll et al., 2002), cell death (Mempel et al., 2006), and cell–cell interactions (Cahalan and Parker, 2008) have been previously observed. Intravital imaging of dendritic cells was first reported in lymph nodes (Mempel et al., 2004; Germain et al., 2006). Myeloid cells have been imaged in a variety of tissues, including the spinal cord and brain (Kim et al., 2009), liver (Geissmann et al., 2005; Egen et al., 2011), kidney (Soos et al., 2006), spleen (Swirski et al., 2009), ear (Auffray et al., 2007), intestine (Chieppa et al., 2006), and recently atherosclerotic arteries (Drechsler et al., 2010; Chèvre et al., 2014; McArdle et al., 2015). Each of these applications share some common traits: the cells of interest must be labeled, the tissue must be stabilized, and the data must be quantitatively analyzed. This review discusses the common methods for each of these steps for imaging myeloid cells, as well as the necessity of incorporating other techniques towards the best interpretation of the data.

Labeling cells

The first step to imaging myeloid cells is to label them with a fluorescent tag. There are two broad categories of labeling techniques: genetic and chemical. In some rare cases, the native autofluorescence of leukocytes has also been used to image them (Li et al., 2010).

Genetic labels

Genetic labeling techniques rely on constructs that report the expression of a gene via a fluorescent protein (FP). GFP and YFP are the most commonly used labels, though mice with cyan fluorescent protein (CFP), or various red fluorescent proteins (RFPs), are available. (Abe and Fujimori, 2013) Engineering reporter mice can be expensive, and it is time-consuming to cross them into other mouse strains. However, once a line is created, no additional work is needed to label every mouse. In some cases, bone marrow transplantation (Stark et al., 2013) or adoptive transfer (Shaked et al., 2015) can be used to label myeloid cells without crossing mice. However, there can be immunological barriers to bone marrow transplantation. Also, the commonly used C57BL/6 recipient mice can reject cells labeled with dsRed protein and some of its derivatives (Davey et al., 2013). An important advantage of genetically labeled cells is that they usually continue to express the fluorescent proteins after long periods of cell culture, or after being adoptively transferred to another mouse. There are a wide range of reporter mice available that are suitable for intravital imaging of myeloid cells, and many have been tested in atherosclerosis (Table 1). Multiple reporters of different fluorescent proteins can be combined, as long as the colors can be spectrally separated (Feng et al., 2000).

To tag a specific subset of cells, it is important to choose both the right gene on which to report, as well as the right type of construct. Traditionally, knock-in mice are made by inserting the cDNA for a fluorescent protein into the natural gene locus, using gene targeting and homologous recombination to replace all or part of the endogenous allele with the cDNA for a fluorescent protein. Knock-in mice made using this method are typically used as heterozygous mice, where one allele encodes the fluorescent protein and the other allele the endogenous protein. This assumes bi-allelic expression (both alleles are expressed in each cell) and haplosufficiency (half the amount of mRNA for the endogenous gene is sufficient for function). Although this is generally true, there can be subtle gene dosage effects on cell function that may not be detected unless specifically scrutinized. For example, monocytes from heterozygous *Cx3cr1*$^{GFP/+}$ mice display an altered phenotype in at least some situations (Combadière et

Correspondence to Klaus Ley: klaus@lji.org

Abbreviations used: 3D, three dimensional; IRES, internal ribosomal entry site; OPO, optical parameter oscillator.

The Rockefeller University Press $30.00
J. Exp. Med. 2016 Vol. 213 No. 7 1117–1131
www.jem.org/cgi/doi/10.1084/jem.20151885

Table 1. **Reporter mice useful for imaging myeloid cells**[a]

Mouse	Approach	Location	Predominant cell types labeled	Original reference	Example papers for intravital imaging of myeloid cells
Cx3cr1^{GFP}	Knock-In	Soluble GFP, cytosolic	Ly6C^{Low} Monocytes, Mac/DC > Ly6C^{Hi} Monocytes	Jung et al., 2000	Athero: Huo et al., 2003 Other: Geissmann et al., 2003
Cd11c^{YFP}	Transgenic	Soluble YFP, cytosolic	Mac/DC (YFP^{hi})	Lindquist et al., 2004	Athero: Li et al., 2010 Other: Coppieters et al., 2010
Lysm^{GFP}	Knock-In	Soluble GFP, cytosolic	Neutrophils > Macrophages, Monocytes	Faust et al., 2000	Athero: Drechsler et al., 2010 Other: Egen et al., 2008
MacGreen *(c-fms)*	Transgenic	Cytosolic GFP	Mac/DC > monocytes neutrophils	Sasmono et al., 2003	Athero: Yu et al., 2007 Other: Looney et al., 2011
Mafia^{GFP} *(c-fms)*	IRES Transgenic	Cytosolic GFP + membrane suicide construct	Mac/DC > monocytes, neutrophils	Burnett et al., 2004	Athero: Chèvre et al., 2014 Other: Peters et al., 2008
MacBlue *(c-fms)*	Transgenic	Cytosolic CFP	Mac/DC > monocytes	Ovchinnikov et al., 2008	Athero: None Other: Sauter et al., 2014
Nr4a1^{GFP}	BAC transgenic	GFP-Cre fusion, mostly nuclear	T cells, Ly6C^{Low} Monocytes	Soriano, 1999	Athero: None Other: Lassailly et al., 2010
MHCII^{GFP}	Knock-in	Fusion Basal-intracellular Activated-surface	Antigen-presenting cells	Boes et al., 2002	Athero: None Other: Varol et al., 2009
CCR2^{RFP}	Knock-in	Cytosolic RFP	Ly6C^{Hi} monocytes	Saederup et al., 2010	Athero: None Other: Jacquelin et al., 2013

[a]The genetic approach, cellular location, major cell types labeled, and examples of their use in intravital imaging of atherosclerotic plaques or other tissues are listed.

al., 2003). When a knock-in reporter mouse is made homozygous (FP/FP), the endogenous gene is knocked out, but continues to express the fluorescent protein. This allows the use of the same mouse strain for reporting and knock-out studies. In the case of the widely used *Cx3cr1*$^{GFP/GFP}$ mouse, it is known that there are defects in Ly6C Low blood monocytes lacking CX_3CR1 (Landsman et al., 2009). Knock-in mice of genes encoded on the X chromosome are knockouts in males. Alternatively, knock-in mice can be made using the internal ribosomal entry site (IRES)–mediated polycistronic reporter system (Bouabe et al., 2008), which allows for simultaneous expression of the targeted gene and the fluorescent protein. This avoids complications caused by loss of the protein of interest.

Knock-in mice typically report the expression of the target gene in the form of cytosolic fluorescence. However, the lifetime of mRNA and protein of fluorescent proteins is rather long, so cells may still be fluorescent after the endogenous protein has been degraded (Chudakov et al., 2010). For instance, the half-life of WT GFP has been measured as 25–54 h (Sacchetti et al., 2001), though modifications can reduce this to 2–5 h (Li et al., 1998; Corish and Tyler-Smith, 1999). Nuclear or other localization signals can be useful to enhance the intensity or change the pattern of fluorescence (Abe and Fujimori, 2013). In some cases, the fluorescent protein is fused directly to the protein of interest to enable tracking of the protein localization (Shaner et al., 2004). This is particularly useful where the gene function is associated with (nuclear or other) relocation, like for NF–κB (De Lorenzi et al., 2009).

Another (older) approach uses transgenic mice produced by pronuclear injection of DNA incorporating the FP cDNA and some part of the promoter (Yang and Gong, 2005). This leads to random insertion into the genome with an unknown copy number. Random integration may disrupt gene expression in the area in which the transgene was inserted. Furthermore, the promoter contains only part of the sequence information needed to impart faithful expression. Gene expression usually also depends on the location within the chromosome (accessible DNA or not), and therefore transgenic reporters usually do not correspond well to the protein of interest (Fig. 1). A newer technique uses a bacterial artificial chromosome (BAC) that inserts the promoter, as well as enhancer elements of the target gene via homologous recombination into a known locus, like *Rosa26*, that has been shown to be constitutively open to transcription (Soriano, 1999). This is better able to accurately report on gene expression (Yang and Gong, 2005).

Unlike knock-in or transgenic reporters, which fluoresce when a gene is being expressed, lineage tracker mice rely on the *Cre/loxP* system to permanently mark cells that have expressed a gene at any point in their lineage (Gu et al., 1994). The Cre recombinase gene is inserted after the locus of the target gene using the IRES system so that both Cre and the original gene are expressed. The Cre recombinase then removes a stop signal surrounded by *loxP* sites, enabling transcription of the gene for a fluorescent protein. Typically, this gene is in the *Rosa26* locus. The cell in which this occurs, and all cells derived from it, will constitutively fluoresce regardless of current gene expression. An additional advantage of lineage tracker mice is that all tagged cells should have similar levels of brightness, because of the constitutive *Rosa26* expression. A variant is the inducible lineage tracker mouse, in which the Cre can be switched on by injecting tamoxifen (Indra et al., 1999). This type of mouse was instrumental in revealing the embryonic origin of macrophages (Yona et al., 2013). Using such mice often shows surprising patterns of gene expression, because Cre recombinase may be activated during a brief bout of gene expression during development that went previously unnoticed.

Another variant of linage tracker mice is the confetti mouse, in which, after Cre recombination, individual cells

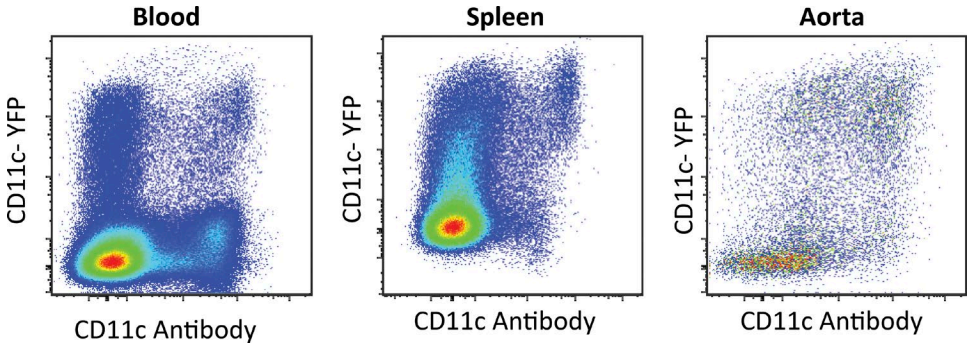

Figure 1. **Representative data showing poor correlation between CD11c surface expression and YFP expression in *Apoe*$^{-/-}$ *CD11c*^{YFP} mice in leukocytes the blood, spleen, and aorta via flow cytometry.** All events gated for live CD45^{+} cells.

stochastically express combinations of CFP, GFP, YFP, and RFP, so that each cell and its derivatives has its own hue (Snippert et al., 2010). Lineage tracker mice have been bred with knock-in mice. For example, in the ex-FoxP3 mice, the cells that currently express the regulatory T cell transcription factor FoxP3 express both GFP and RFP, whereas cells that expressed FoxP3 in their past but not currently express only RFP (Miyao et al., 2012).

Cells in functional reporter mice become fluorescent after the activation of a specific function instead of simply as a marker of the cell subset. For instance, in the *Nr4a1*^{GFP} mouse, T cells increase GFP brightness after TCR activation (Moran et al., 2011). In p65^{GFP} mice, GFP is expressed cytosolically in many cell types, but is translocated into the nucleus after NF–κB pathway activation (De Lorenzi et al., 2009). Nuclear translocation is an excellent indicator of activation and has the added benefit that the cell is visible by fluorescence microscopy before and after activation. Functional reporters can be generated from any of the aforementioned genetic engineering techniques, depending on the biological question.

Another class of mice with fluorescent cellular tags useful for imaging express a photoconvertible fluorescent protein, such as Kaede (Tomura et al., 2008), Kikume-Green Red (Tomura et al., 2014), or other forms of photoactivatable-GFP (Patterson and Lippincott-Schwartz, 2002; Victora et al., 2010). These photoconvertible proteins change their emission spectra (or, in the case of GFP, their excitation spectra) after being excited with a specific wavelength of light (Abe and Fujimori, 2013). This can be used to mark cells in one location and then trace how cells traffic throughout the body. The Kaede and Kikume-Green mice can also be used to differentiate cells that have immigrated into the tissue after a photoconversion took place (Tomura et al., 2008). The protein conversion is stable (permanent in the case of Kaede and Kikume-Green, up to 1 wk for photoactivatable GFP), but the cell can still synthesize new, unconverted fluorophores, limiting the time in which the photoconversion is reliably detectable (Tomura et al., 2008). Cell division will dilute the converted protein. Recently, a mouse was developed that expresses a photoinducible Cre that drives tdTomato expression, allowing cells to be permanently labeled by exposing them to blue light (Schindler et al., 2015). A two-photon microscope can provide precision excitation, though only a small number of cells can be photoconverted (Chtanova et al., 2014), which leads to difficulty finding the cells later. Alternatively, a UV lamp can convert whole sections of tissue simultaneously (Schulz et al., 2014).

Limitations

An overview of reporter mice that have been used in intravital imaging of myeloid cells in atherosclerosis or other systems are listed in Table 1, along with their approach, cellular location, and major cell types labeled. An in-depth study of the details of each of these reporter mice and how they have been used is beyond the scope of this review. However, some examples can demonstrate the importance of experimentally confirming which cells are labeled (specificity) and what percentage of the target cells are labeled (yield). When a reporter mouse is first made, the target cell is reported to be tagged with a certain efficiency, but in later studies, more cell types are found to be also tagged. As a case in point, *Cd11c*^{YFP} mice were originally made to visualize myeloid dendritic cells, and this works well in lymph nodes (Lindquist et al., 2004). However, it was later shown by flow cytometry that in atherosclerotic plaques, YFP expression does not correlate well to surface CD11c expression (Fig. 1; Koltsova et al., 2012). Using cytospin and fluorescence microscopy, it was shown only the brightest cells are visible by microscopy, and those are the only ones that can be considered dendritic cells in atherosclerotic plaques (Koltsova et al., 2012). In *Lysm*$^{GFP/GFP}$ mice, neutrophils are brightest, but monocytes and macrophages are still visible in some systems (Faust et al., 2000). In the very commonly used *Cx3cr1*^{GFP} mouse, GFP expression has been reported in a wide variety of cell types, including both subsets of monocytes (Geissmann et al., 2003), NK cells, neutrophils, T cells (Mionnet et al., 2010), myeloid precursors (Fogg et al., 2006; Liu et al., 2009), and various tissue macrophages and dendritic cells (Jung et al., 2000; Swirski et al., 2009; Varol et al., 2009; Bar-On et al., 2010; Jacquelin et al., 2013; Lionakis et al., 2013). These examples support our opinion that the

proper approach to fluorescent cell imaging in vivo is to identify the labeled cells and characterize them by flow cytometry, immunohistochemistry, and transcriptomic analysis.

Chemical labels

Chemical labels are immediately available and do not require any mouse crossing. Most types are available in a wider variety of colors than genetic labels. Some chemical labels show more photobleaching (Shaner et al., 2005) and are more sensitive to tissue processing methods than genetically labeled cells, although soluble fluorescent proteins can be easily washed away during processing and can be hard to detect in tissue sections. One of the simplest methods is to inject a fluorescently labeled antibody into the mouse. This works well for antigens with high surface expression, such as Ly-6G (Shaked et al., 2015), but antibodies cannot be used to detect intracellular antigens in live cells. Antibodies will quickly label cells in the blood (Shaked et al., 2015), but can take hours to diffuse into tissue (Wang et al., 2014). Therefore, the experimental protocol must be optimized to ensure that the entire tissue being imaged is adequately exposed to antibody but that it has not yet cleared from the body. Tissues with inadequate blood flow, including advanced atherosclerotic plaques and necrotic cores of tumors, are difficult to label via intravenous antibody injection. Injecting high quantities of labeled antibody can in fact be used to mark the blood volume (Shaked et al., 2015) for short-term experiments. A more targeted approach via injection of the antibody into the tissue has been successfully used, e.g., to label lymphatic vessels in the leg and draining lymph node. Antibodies labeled with fluorescent proteins, such as phycoerythrin or allophycocyanin, photobleach quickly under conditions of multiphoton microscopy, but recent advances in organic dyes, (i.e., the Alexa Fluor family and the DyLights Fluor family, among others) are improving imaging time (Johnson, 2006).

As with reporter mice, it is important to confirm in every imaged tissue that that the antibody is marking the cells of interest with high yield and high specificity. Specificity can be confirmed with appropriate negative controls. The ideal negative control is to use the antibody on a mouse that is deficient for the protein of interest. Other controls include imaging the sample before labeling to observe any autofluorescence, simultaneous injection of an isotype control in a different color to look for nonspecific or Fc-receptor–mediated bind, or (for compartments like blood that show very fast labeling), injecting an isotype control in the same color first, and (only after observing no binding) applying the experimental antibody. The labeling efficiency of the cells of interest can be calculated by analyzing the tissue after injection with flow cytometry. When possible, one should try to observe the cells with and without antibody labeling to determine if the antibody blocks the function of the ligand protein and therefore interferes with cell motion. Some antibodies deplete blood cells; for example, high concentrations of Ly-6G antibodies deplete neutrophils (Daley et al., 2008), NK1.1 depletes NK and NKT cells (Koyama, 2002), and GPIbα antibodies deplete platelets (Iannacone et al., 2005). In each case, the concentration of antibody needed to label or deplete the cells of interest must be determined in preliminary experiments.

The phagocytic activity of myeloid cells can be harnessed to label and track them in vivo, without external handling. Cells (predominantly blood monocytes) phagocytose injected fluorescently labeled beads, and then carry them as they transmigrate into tissue or differentiate into macrophages/dendritic cells (Tacke et al., 2007). This technique has yielded valuable insights into the origin and trafficking of macrophages in atherosclerotic lesions (Tacke et al., 2007; Potteaux et al., 2011), though its use in intravital imaging has thus far been limited (Haka et al., 2012). In other studies, labeled high-molecular weight dextran has been used as an in vivo phagocytosis substrate to identify macrophages (Wyckoff et al., 2007). With these techniques, it is important to test for cell activation after the phagocytosis (Tacke et al., 2007). Additionally, it is important to consider transfer of the marker to an unlabeled macrophage that phagocytosed an apoptotic labeled cells (Ahrens et al., 2005; Sutton et al., 2008). This occurs when macrophages phagocytose dead labeled monocytes in atherosclerotic plaques (Potteaux et al., 2011). In some cases, myeloid cells can fuse (McNally and Anderson, 2011), sharing the label and further complicating data interpretation (Davies et al., 2009).

If direct labeling in vivo is not feasible, adoptive transfer of labeled cells may be a good option. This approach has been successful for monocytes (Hanna et al., 2015) and neutrophils (Zinselmeyer et al., 2008). Cytosolic labels that passively diffuse through the cell membrane come in a variety of classes with different chemical properties and retention times (Parish, 1999; Johnson, 2006). Some (e.g., calcein-AM) have an acetoxymethyl ester group that is cleaved, trapping it inside the cytosol. Cells can actively pump these out, and in some cases they are only retained for a few hours, and thus are usually best suited for short-term experiments. Others, like CFSE or CMRA, covalently bind to intracellular and extracellular proteins, and remain in the cell for days. These provide even labeling of the cell that will dilute with cell division (Progatzky et al., 2013). The dilution effect can be used to track the number of cell divisions up to the level where the limit of detection is reached. Unlike flow cytometry, microscopy can only resolve one or two divisions reliably because of the limited dynamic range and the loss of fluorescence intensity with depth. A major disadvantage to these dyes is that they can be cytotoxic (Last'ovicka et al., 2009).

An alternative to cytosolic labels are membrane labels, which have been reported to be less cytotoxic (Horan and Slezak, 1989). Intercalating membrane labels, including the DiI, O, D, and R series and the PKH series (Parish, 1999; Poon et al., 2000; Sundd and Ley, 2013), are easy to use and integrate spontaneously but they can jump from the target cell to other cells (Lassailly et al., 2010; Li et al., 2013). Macrophages are particularly likely to pick up dyes from adop-

tively transferred cells (Pawelczyk et al., 2009; Progatzky et al., 2013). PKH26 is noteworthy, as it stays on the cell for weeks to months (Parish, 1999). Membrane dyes have the advantage of specifically labeling the borders of cells, which can be useful for separating touching cells. Nuclear dyes can also help distinguish densely packed cells. Hoechst 33342 labels live cells and is suitable for tracking cell migration because it is bright and resistant to photobleaching (Mempel et al., 2006). However, it is known to interfere with cell replication (Parish, 1999). After being labeled by any of these methods, cells can be injected into the blood to circulate systemically, into the foot pad to reach the draining popliteal lymph node, or in other locations (e.g., intraperitoneal).

Adoptive transfer of differentially labeled cells can be used to study the motion of different groups (WT vs. KO, control vs. treated, two different subsets) simultaneously under identical conditions. This helps to ensure that any differences observed between groups are caused by the labeled cells and not different environments or surgical preparations (Lämmermann and Germain, 2014). Whenever differential labeling is used, it is essential that a color-switching control is performed to ensure there are no dye-specific effects. In addition, all exogenous labeling methods require cells to be handled in vitro. Myeloid cells are easily activated by handling outside the mouse, and this activation must be accounted for when interpreting data (Lyons et al., 2007).

Experimental set-up

The main challenge in intravital microscopy is to image the cells of interest without undue tissue damage (surgical access needed for most tissues) or excessive motion artifacts (heartbeat, breathing). The choice of microscope depends on the biological question being asked. Upright microscopes are best suited for most intravital experiments. For imaging brightly labeled cells in the microcirculation, especially in thin tissues like the cremaster muscle, epifluorescence microscopy is often sufficient (Ley et al., 1995). This simple method enables fast acquisition with a large field-of-view but is limited to two-dimensional images. However, these limitations are acceptable for imaging myeloid cells crawling along blood vessels. In fact, this technique has even been used to image monocytes adhering to healthy and mildly diseased carotid arteries (Huo et al., 2003; Chèvre et al., 2014). This technique is compatible with stroboscopic illumination that effectively freezes all tissue motion (Huo et al., 2003). Double stroboscopic illumination allows direct measurement of the velocity of free-flowing cells in the blood (Norman et al., 1995; Smith et al., 2003).

For imaging deeper into tissue, including arteries with advanced atherosclerotic plaques, techniques that provide three-dimensional resolution are needed. Confocal microscopy has many benefits, including higher lateral and axial resolution than epifluorescence, especially in optically dense tissues, and, in most systems, the ability to simultaneously collect multiple channels excited by multiple lasers. Spinning-disk confocal microscopy can acquire images at a faster frame rate than that of laser scanning confocals, but at the cost of decreased spatial resolution, lower brightness, and lower signal-to-noise ratio. Resonant scanners greatly improve the acquisition speed of laser-scanning microscopes, both confocal and multiphoton. Both types of confocal microscopy are limited in penetration depth to ∼50 µm.

Two-photon excitation provides better penetration depth, and so is routinely used in intravital imaging (Mempel et al., 2004). It also produces less photobleaching and phototoxicity than confocal microscopy (Potter et al., 1996). Two-photon microscopes can acquire images at the same rate as laser-scanning microscopes. The lateral resolution of two-photon microscopy is slightly lower than that of laser scanning confocal but the axial resolution is much worse. However, for tracking cell motion, even that of projections of dendritic cells, the resolution is typically sufficient (Li et al., 2010; Koltsova et al., 2012). Additionally, two-photon microscopy allows label-free imaging of collagen, a major extracellular matrix component, via second harmonic generation (Zoumi et al., 2002). The effective imaging depth is up to 200 µm, and there is significant attenuation because of absorption and scattering such that cells deep in the tissue appear dimmer and more elongated than superficial cells. Most two-photon microscopes with a TI:sapphire laser have difficulty exciting red and far-red fluorophores like RFP and allophycocyanin. Typically only one excitation wavelength can be used at a time, limiting the range of fluorophores than can be imaged simultaneously. Switching excitation wavelengths takes seconds, and therefore is only practical for cells which are moving slowly. An optical parameter oscillator (OPO) can extend the excitation range into the infra-red spectrum, up to 1500 nm, allowing deeper penetration and excitation of red and far-red dyes (Vadakkan et al., 2009; Zal and Chodaczek, 2010). In fact, use of an OPO combined with red fluorescent proteins has increased penetration depth to almost 1 mm in intravital imaging (Kobat et al., 2009). It can also allow for multiple simultaneous excitation wavelengths (Herz et al., 2010), though switching between excitation wavelengths is still best for spectral separation (Zal and Chodaczek, 2010). With use of an OPO, third harmonic generation can be used to visualize lipid–water interfaces (Friedl et al., 2007).

Surgical set-up

Accessing the desired organ often requires delicate surgery of an anesthetized mouse; only a few tissues like the mouse ear (Auffray et al., 2007; Li et al., 2012a) are accessible without surgery. To get physiologically relevant results, it is important to not damage the imaged tissue or to restrict blood flow to the area. First, the mouse and the imaged tissue must be kept near physiological temperature, pH, and osmolarity for optimal cell motion (Miller et al., 2002). A blood tracer (i.e., Evans blue, labeled dextran, or quantum dots) can be injected i.v. to test for vascular leakage (Li et al., 2012a). These same tracers can be injected into areas with well-defined draining

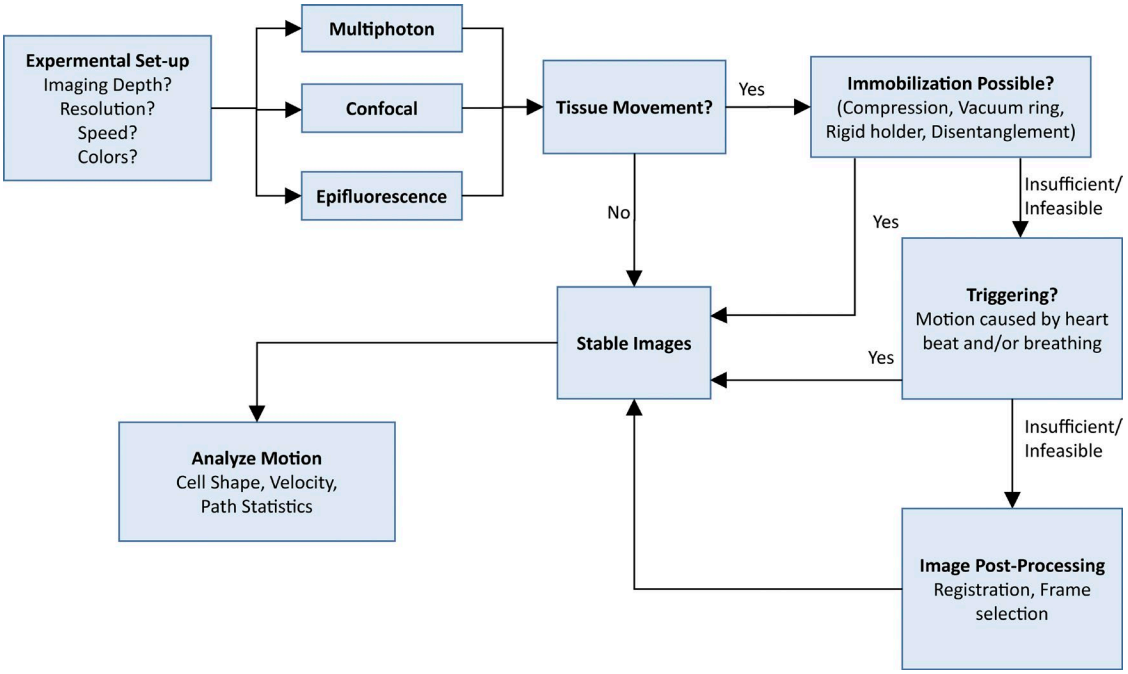

Figure 2. **Decision flow chart for acquiring intravital videos.** The choice of microscope depends mainly on the imaging depth (multiphoton better), resolution and colors (confocal better) or speed (epifluorescence better, see text for details). If tissue motion causes artifacts, mechanical immobilization, cardiac, and/or respiratory triggering, and image postprocessing can be used to stabilize the images, and then cell motion can be analyzed.

lymph nodes (i.e., the footpad for the popliteal and the ear or base of the neck for the cervical lymph node) to check for intact lymphatic drainage to those lymph nodes (Zinselmeyer et al., 2009). Red blood cells flowing through capillaries are a good indicator of microvascular perfusion (Bagher and Segal, 2011). In some systems, the velocity profile of free-flowing red blood cells can be calculated for a more sensitive measurement (Fumagalli et al., 2014). Recruitment of leukocytes is a sign of local inflammation; this can be easily visualized in $Lysm^{GFP}$ mice (Lämmermann et al., 2013). Unusually low cell motility is a sign of tissue damage (Zinselmeyer et al., 2009) and propidium iodide can be used to identify dead cells (Megens et al., 2010). Passing these tests suggests that the surgical preparation was not detrimental, but intravital microscopy inherently remains an invasive technique. It is best to disturb the tissue as little as possible, as some groups have found that observed cell functions are altered with more aggressive surgical preparations (McDole et al., 2012).

Motion artifacts

Motion artifacts constitute a large technical challenge in intravital imaging. The most common sources of tissue motion are the mouse's breathing and heartbeat, which can affect nearly all organs in the thoracic and peritoneal cavities. Various set-ups have been designed to isolate tissues from breathing motion, while maintaining a physiological environment (Mempel et al., 2004; Coppieters et al., 2010; Marker et al., 2010; McDole et al., 2012; Jenne et al., 2013; Kolaczkowska et al., 2015). However, these simple isolation systems do not sufficiently stabilize organs with inherent motion, such as the lungs, heart, or large arteries. For these tissues, more complicated systems have been devised (Fig. 2).

There are three commonly used methods for minimizing motion artifacts in intravital imaging of tissues with innate motion: mechanical stabilization, image post-processing, and triggering (Vinegoni et al., 2014). Various techniques (tissue glue, suction ring, compression) have been successfully used for physically restraining tissue movement (Looney et al., 2011; Lee et al., 2012a,b; Li et al., 2012b; Vinegoni et al., 2012; Jung et al., 2013; Chèvre et al., 2014). As described above, it is important to ensure that placing the stabilizer does not induce any tissue damage. One alternative that minimizes physical stress on the tissue is to freely acquire a large amount of data and then use post-processing to select only a fraction of the data for further analysis (Drechsler et al., 2010; Lee et al., 2012a; Soulet et al., 2013). Frame or pixel selection can be automated for large amounts of data (Vinegoni et al., 2014; McArdle et al., 2015), or individual frames can be chosen by hand (Drechsler et al., 2010). Post-processing can also include image registration to remove small translation or rotation artifacts (Ray et al., 2015). Because this method relies on acquiring more data than is used, the tissue is exposed to excess excitation light, which will increase photobleaching. In an alternative method, triggering, image acquisition is synchronized to the mouse's heartbeat, breathing cycle, or both. The acquisition is timed to occur during the point in each cycle

when the tissue is moving the least. Triggered imaging allows for high-resolution imaging with minimal photobleaching by only exposing the tissue to excitation light when it is in a quasi-steady position (Megens et al., 2010; Chèvre et al., 2014). Obtaining apparent stability is only possible if the mouse maintains a consistent heart rate and stable breathing, which requires a steady level of anesthesia and good surgical technique. Even then, some visible tissue motion is unavoidable. Triggering is often combined with mechanical stabilization or image post-processing to further improve movie quality (Lee et al., 2012a,b; Vinegoni et al., 2012, 2013; Chèvre et al., 2014; McArdle et al., 2015). We have developed a software suite that automatically selects the best frames and performs rigid body registration that is freely available (McArdle et al., 2014, 2015; Ray et al., 2015).

Analyzing imaging data

There is a large amount of information that can be acquired about cells from intravital imaging: e.g., motion, migration, shape change, division, phagocytosis, and antigen presentation. The most common analysis technique is tracking the migration of the entire cell body. From there, the density of crawling/patrolling cells and their velocity alongside track length, direction, and confinement ratio (ratio of path length to net distance traveled) can be calculated and qualitatively described (Miller et al., 2003; Sumen et al., 2004; Auffray et al., 2007). Monitoring changes in cell body motion has been instrumental in working out environmental cues and molecular mechanisms involved in the leukocyte adhesion cascade (Ley et al., 2007), monocyte patrolling, and arrest (Huo et al., 2001; Auffray et al., 2007; Carlin et al., 2013), and transmigration (Phillipson et al., 2006). Neutrophil transmigration into atherosclerotic plaque was demonstrated (Chèvre et al., 2014), and monocytes were shown to patrol the atherosclerotic endothelium (Li et al., 2010), though monocyte transmigration has not yet been observed.

Within tissues, cells tend to migrate more slowly than in blood vessels, and other cell functions can be observed. Uptake of damaged cells (Evans et al., 2014), bacteria (Chieppa et al., 2006), and environmental antigens (Wyckoff et al., 2007; McDole et al., 2012) by macrophages has been observed in various tissue. In these studies, the substrate being phagocytosed was fluorescent, and the myeloid cell was visualized taking up pieces of fluorescent material. The shape of the cell can give information about it status; for instance, microglia lose their processes and become rounded when activated (Aloisi, 2001; Shaked et al., 2015). In other studies, macrophages and DCs were seen probing their environment, sometimes through epithelial monolayers (Soos et al., 2006; McDole et al., 2012; Barkauskas et al., 2013; Krabbe et al., 2013; Engel et al., 2015). Within atherosclerotic plaques of *Cx3cr1*$^{GFP/+}$ *Cd11c*^{YFP} *Apoe*$^{-/-}$ mice, GFP$^+$, YFP$^+$, and GFP$^+$YFP$^+$ cells have been observed migrating through the plaque and "dancing on the spot," which means extending and retracting dendritic processes (McArdle et al., 2015). It is unclear what function this behavior represents. This dancing or probing behavior can be quantified by various measurements, including dendricity index, shape retention index, and dendrite velocity (Baxter et al., 1991; Chodaczek et al., 2012). Having bright markers is important for these measurements, because the small diameter of dendrites (~1 μm) makes them dimmer than the cell body. Additionally, the microscope must be able to spatially resolve these features. In general, water immersion objectives with a numerical aperture close to 1.0 provide excellent resolution for intravital microscopy (Shaner et al., 2005; Ley et al., 2008).

Intravital imaging can reveal cell–cell interactions that are essential to many homeostatic or inflammatory processes. Patrolling monocytes interacting with fluorescent tumor cells were shown to reduce tumor metastasis (Hanna et al., 2015). Intravital imaging of leukocytes adhering to each other in blood flow was essential to understanding secondary capture (Kunkel et al., 1998). Antigen presentation has been demonstrated by observing contact between T cells and dendritic cells (Miller et al., 2002; Stoll et al., 2002; Mempel et al., 2004; Milo et al., 2013). Similar results were demonstrated in atherosclerotic aorta explants (Koltsova et al., 2012), although antigen presentation remains to be observed in atherosclerotic plaques in vivo.

Intravital imaging of atherosclerotic arteries

Intravital imaging of leukocytes in atherosclerotic arteries is still a developing field. The first work was published in 2011 using epifluorescence microscopy (Megens et al., 2011). Though this technique provides low lateral and no axial resolution, it was invaluable in early work on the activity of leukocytes near atherosclerotic plaques. Monocytes were visualized tethering to, rolling on, and adhering to atherosclerotic lesions in the carotid artery in a P-selectin–dependent manner (Huo et al., 2003). Similarly, neutrophil rolling on the abdominal aorta was found to depend on both P- and E-selectin (Eriksson et al., 2001a). Epifluorescence microscopy was also instrumental in determining the role of secondary capture in atherosclerosis (Eriksson et al., 2001b). Multicolor epifluorescence microscopy of mechanically stabilized carotid arteries was used to quantify rolling in multiple leukocyte subsets at different stages of the disease, as well as the polarization of crawling cells in Mafia^{GFP} mice, which have fluorescent myeloid cells (Chèvre et al., 2014). The effect of blocking various chemokine receptors on neutrophil recruitment to plaques was also assayed by epifluorescence microscopy (Drechsler et al., 2010).

Proof-of-concept of two-photon imaging of leukocytes in atherosclerotic arteries in vivo was published in 2004 (van Zandvoort et al., 2004), although the images were distorted by vessel motion. A single z-stack of GFP-labeled myeloid cells in the carotid artery wall of a MacGreen mouse, with labeled myeloid cells, was published in 2007 using a system that severely stretched the vessel to inhibit all motion (Yu et al., 2007). Single frames from freely expanding arteries imaged with a fast scanner were used to quantify the diameter of

and blood flow velocity through vasa vasorum microvessels of atherosclerotic carotid artery (Rademakers et al., 2013).

It was not until 2010 that two-photon videos of high enough quality to allow cell tracking were published. Neutrophils were tracked for 30 min in a single *Lysm*$^{GFP/GFP}$ *Apoe*$^{-/-}$ mouse as they crawled along the endothelium, changed shape, and potentially transmigrated into the plaque (Drechsler et al., 2010). In this work, only a single plane was imaged and frames were manually selected for further analysis. The same year, cardiac and respiratory triggering was used to image unidentified leukocytes labeled with SYTO13 crawling in the healthy carotid artery wall (Megens et al., 2010). However, the mouse was reported to have low blood pressure and it is unclear what effect this had on the cells. Only a single plane was imaged, making three-dimensional (3D) tracking impossible. Later, a combination of mechanical stabilization and respiratory triggering was used to acquire videos of neutrophils adherent to the carotid artery wall of a *Lysm*$^{GFP/GFP}$ *Apoe*$^{-/-}$ mouse (Chèvre et al., 2014). The authors used 3D imaging, as well as a blood volume label and second-harmonic imaging of collagen to confirm the location of the cells. In 2015, monocytes and macrophages were imaged in atherosclerotic arteries of *Cx3cr1*$^{GFP/+}$ *Cd11c*^{YFP} *Apoe*$^{-/-}$ mice using ILTIS, a system that relies on cardiac triggering, followed by image selection and registration to remove residual artifacts (McArdle et al., 2015). Single plane imaging was used to show GFP$^+$ monocytes patrolling along the external carotid artery endothelium both with and against blood flow for up to 45 min, the first report of this behavior in atherosclerosis. Within the arterial wall, GFP$^+$ and GFP$^+$YFP$^+$ cells were seen dancing on the spot using 3D imaging. Dendritic projections from two cells were tracked as they extended and appeared to interact with each other. Simultaneously, rounded YFP$^+$ cells were tracked in 3D as they migrated through the plaque.

Combining with other techniques

As discussed above, intravital imaging must always be paired with other analysis techniques to properly identify and characterize the imaged cells (Fig. 3). A common way to determine the phenotype of the labeled cells is to digest the tissue of interest, and then perform flow cytometry. Conventional four-laser flow cytometry allows the distinction of ∼15-17 colors and requires proper negative controls and compensation. Negative controls include testing for nonspecific binding by replacing the antibody with a labeled isotype control or by analyzing cells from a mouse lacking the analyzed receptor. Fluorescence-minus-one (FMO) controls, where all colors except one are used, can test for bleed-through from other channels or autofluorescence (Herzenberg et al., 2006). Mass cytometry, or CyTOF, can theoretically resolve >100 isotopes, without needing any compensation (Giesen et al., 2014). CyTOF is currently limited by the limited availability of lanthanides (∼40) and conjugated antibodies. A disadvantage of this technique is that it is necessarily destructive to the cell, and thus the cells cannot be used for sorting, mRNA isolation, or transcriptomics. Single-cell suspensions can be stained for commonly accepted lineage markers, i.e., CD45 for leukocytes, CD11b for most myeloid cells; CD115 and Ly6C for monocytes; Ly6G and Ly6C for neutrophils; F4/80, CD64, and MerTK for macrophages in most tissues, and CD11c for dendritic cells and inflammatory M1 macrophages. A dump channel (for example, CD19, CD3, and NK1.1) is used to exclude all nonmyeloid cells. Additionally, one can stain for the presence of surface markers for specific cell functions, such as chemokine receptors, scavenger receptors, or MHCII, which predicts the ability to present peptide antigens to CD4 T cells. Antibody labeling of intracellular proteins, like transcription factors, is impossible during intravital microscopy, but can yield useful information via flow cytometry. Common targets include pro- and antiinflammatory cytokines and chemokines, iNOS and Arginase 1 to distinguish M1 vs M2 macrophages, and Ki67 or BrDU to label proliferating cells. For cells that only dimly express GFP or YFP, intracellular anti-GFP antibodies can be used to improve the signal. Cytosolic fluorescent proteins are sometimes lost during fixation and permeabilization for intracellular or nuclear epitopes. This can largely be prevented by prefixing the cells with paraformaldehyde (Grupillo et al., 2011). Combining many markers in one experiment gives the best information about the range of cells in the population.

Fluorescently labeled cells from single-cell suspensions can be sorted by flow cytometry to conduct global analysis of the imaged cells. This includes analysis of gene expression by RNA-Seq (Broz et al., 2014) or microarray (Laguna and Alegret, 2012), transcription factor–binding sites and histone modifications by ChIP-Seq (Gosselin et al., 2014), accessible chromatin regions by ATAC-Seq (Lavin et al., 2014), and protein expression by LC-MS/MS proteomics (Le Faouder et al., 2013). Fluorescently labeled cells can be sorted into a cytospin to test the lower threshold of brightness that can be visualized by the microscope (Koltsova et al., 2012). This is an estimate only, because the actual brightness that is detectable also depends on the attenuation by the scan depth (z position) and tissue composition. Cells that have been plated on cover glass-bottom dishes or cytospun can be analyzed for shape to help determine their phenotype, though this can also be performed on an imaging flow cytometer (Majka et al., 2012). Sorted cells can also be used for in vitro functional assays like antigen presentation (Choi et al., 2009), cytokine production by cytometric bead array (Morgan et al., 2004), phagocytosis (Xu et al., 2010), efferocytosis of apoptotic cells (Friggeri et al., 2010), and killing of pathogens (Drevets et al., 2015).

Tissue digestion for flow cytometry or sorting removes information about the location of the labeled cells, their neighbors, and their microenvironment and can remove certain protease-sensitive cell surface antigens (Autengruber et al., 2012). In many cases, enzymatic digestion does not retrieve all cell subsets equally (Gerner et al., 2012). Immunofluorescence can be performed on tissue with cells with genetic or some chemical labels, but some others are sensitive

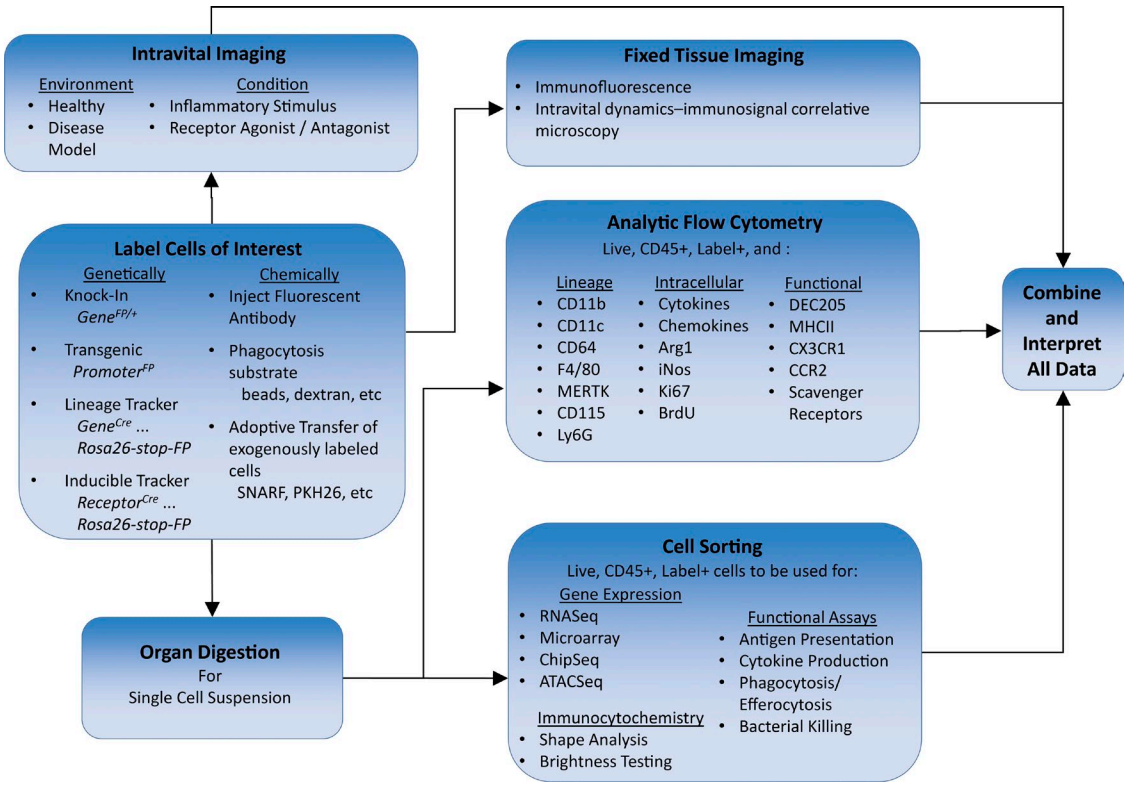

Figure 3. **Determining phenotype and function of myeloid cells by combining intravital imaging with other techniques.** Cells of interest are first labeled, either genetically with reporter mice or chemically, to be imaged in vivo. The labeled cells must also be analyzed with other techniques such as fixed tissue imaging, analytic flow cytometry for lineage and functional markers, functional assays, or gene expression. Finally, all data are combined for analysis and interpretation.

to fixation. Perfusion fixation performed in situ immediately after the mouse is sacrificed best preserves tissue structure, though fixation can be performed after the organ is removed, if necessary. When working with genetically labeled cells with cytosolic fluorescent protein it is imperative to fix the tissue before any sectioning; otherwise, the signal will be lost. Fixed tissue sections can be stained for the lineage and functional markers mentioned above for flow cytometry, though typically only ∼4-5 colors can be imaged simultaneously. Recent work in histocytometry has enabled precise quantification of up to eight labels with confocal microscopy (Gerner et al., 2012). Immunofluorescence enables analysis of the location of the target cells within the tissue, their shape, and what other cell types they are interacting with.

Whole-mount immunofluorescence, where antibodies are applied directly to small pieces of fixed tissue without sectioning, is becoming more common (Yokomizo et al., 2012). This technique nicely complements intravital microscopy, because it allows higher resolution imaging with no motion artifacts, whereas intravital imaging reveals cell dynamics. Whole-mount imaging preserves tissue structure, which can be damaged by sectioning. With novel optical clearing protocols that remove lipids and other causes of light scattering from the sample up to 5 mm of depth penetration is possible, to enable a more comprehensive look at the tissue as a whole (Tomer et al., 2014; Susaki et al., 2015). Whole-mount imaging is used in an informative technique called intravital dynamics-immunosignal correlative microscopy (Chodaczek et al., 2012). In this technique, after intravital imaging, the specimen is fixed and whole-mount immunofluorescence staining for relevant proteins is performed. Then, the specimen is mounted on a slide, and the area that had been imaged can be found. The specific cells that were observed can be deeply analyzed, along with their surroundings, and that data can be correlated to their intravital motion. This allows for deeper investigation of the causes and mechanisms of cell motion.

Conclusion

Intravital microscopy has come a long way from humble beginnings using white light transillumination of transparent tissues (Wagner, 1839). Today, intravital imaging with multicolor multiphoton microscopy is giving us insights into the dynamics of healthy and diseased tissues that have never before been possible. Atherosclerosis is just one of the rich biological areas that are progressing rapidly through the use of these techniques. Although intravital imaging of myeloid cells has become more reliable in recent years, many systems are still hampered by artifacts caused by tissue motion and imprecise

cell labeling. However, by combining triggered acquisition, automated frame selection, and image registration, motion artifacts can be minimized. Furthermore, the addition of transcriptomics, flow cytometry, and immunofluorescence allows for more precision when interpreting intravital imaging for biological meaning. By combining these techniques, we can truly begin to understand cellular dynamics in living tissue.

ACKNOWLEDGMENTS

The authors declare no competing financial interests.

Submitted: 2 December 2015
Accepted: 28 April 2016

REFERENCES

Abe, T., and T. Fujimori. 2013. Reporter mouse lines for fluorescence imaging. *Dev. Growth Differ.* 55:390–405. http://dx.doi.org/10.1111/dgd.12062

Ahrens, E.T., R. Flores, H. Xu, and P.A. Morel. 2005. In vivo imaging platform for tracking immunotherapeutic cells. *Nat. Biotechnol.* 23:983–987. http://dx.doi.org/10.1038/nbt1121

Aloisi, F. 2001. Immune function of microglia. *Glia.* 36:165–179. http://dx.doi.org/10.1002/glia.1106

Auffray, C., D. Fogg, M. Garfa, G. Elain, O. Join-Lambert, S. Kayal, S. Sarnacki, A. Cumano, G. Lauvau, and F. Geissmann. 2007. Monitoring of blood vessels and tissues by a population of monocytes with patrolling behavior. *Science.* 317:666–670. http://dx.doi.org/10.1126/science.1142883

Autengruber, A., M. Gereke, G. Hansen, C. Hennig, and D. Bruder. 2012. Impact of enzymatic tissue disintegration on the level of surface molecule expression and immune cell function. *Eur. J. Microbiol. Immunol.* 2:112–120. http://dx.doi.org/10.1556/EuJMI.2.2012.2.3

Bagher, P., and S.S. Segal. 2011. The mouse cremaster muscle preparation for intravital imaging of the microcirculation. *J. Vis. Exp.* 52:2874.

Barkauskas, D.S., T.A. Evans, J. Myers, A. Petrosiute, J. Silver, and A.Y. Huang. 2013. Extravascular CX3CR1$^+$ cells extend intravascular dendritic processes into intact central nervous system vessel lumen. *Microsc. Microanal.* 19:778–790. http://dx.doi.org/10.1017/S1431927613000482

Bar-On, L., T. Birnberg, K.L. Lewis, B.T. Edelson, D. Bruder, K. Hildner, J. Buer, K.M. Murphy, B. Reizis, and S. Jung. 2010. CX3CR1$^+$ CD8α^+ dendritic cells are a steady-state population related to plasmacytoid dendritic cells. *Proc. Natl. Acad. Sci. USA.* 107:14745–14750. http://dx.doi.org/10.1073/pnas.1001562107

Baxter, C.S., A. Andringa, K. Chalfin, and M.L. Miller. 1991. Effect of tumor-promoting agents on density and morphometric parameters of mouse epidermal Langerhans and Thy-1+ cells. *Carcinogenesis.* 12:1017–1021. http://dx.doi.org/10.1093/carcin/12.6.1017

Boes, M., J. Cerny, R. Massol, M. Op den Brouw, T. Kirchhausen, J. Chen, and H.L. Ploegh. 2002. T-cell engagement of dendritic cells rapidly rearranges MHC class II transport. *Nature.* 418:983–988. http://dx.doi.org/10.1038/nature01004

Bouabe, H., R. Fässler, and J. Heesemann. 2008. Improvement of reporter activity by IRES-mediated polycistronic reporter system. *Nucleic Acids Res.* 36:e28. http://dx.doi.org/10.1093/nar/gkm1119

Broz, M.L., M. Binnewies, B. Boldajipour, A.E. Nelson, J.L. Pollack, D.J. Erle, A. Barczak, M.D. Rosenblum, A. Daud, D.L. Barber, et al. 2014. Dissecting the tumor myeloid compartment reveals rare activating antigen-presenting cells critical for T cell immunity. *Cancer Cell.* 26:638–652. http://dx.doi.org/10.1016/j.ccell.2014.09.007

Burnett, S.H., E.J. Kershen, J. Zhang, L. Zeng, S.C. Straley, A.M. Kaplan, and D.A. Cohen. 2004. Conditional macrophage ablation in transgenic mice expressing a Fas-based suicide gene. *J. Leukoc. Biol.* 75:612–623. http://dx.doi.org/10.1189/jlb.0903442

Cahalan, M.D., and I. Parker. 2008. Choreography of cell motility and interaction dynamics imaged by two-photon microscopy in lymphoid organs. *Annu. Rev. Immunol.* 26:585–626. http://dx.doi.org/10.1146/annurev.immunol.24.021605.090620

Carlin, L.M., E.G. Stamatiades, C. Auffray, R.N. Hanna, L. Glover, G. Vizcay-Barrena, C.C. Hedrick, H.T. Cook, S. Diebold, and F. Geissmann. 2013. Nr4a1-dependent Ly6C(low) monocytes monitor endothelial cells and orchestrate their disposal. *Cell.* 153:362–375. http://dx.doi.org/10.1016/j.cell.2013.03.010

Chèvre, R., J.M. González-Granado, R.T. Megens, V. Sreeramkumar, C. Silvestre-Roig, P. Molina-Sánchez, C. Weber, O. Soehnlein, A. Hidalgo, and V. Andrés. 2014. High-resolution imaging of intravascular atherogenic inflammation in live mice. *Circ. Res.* 114:770–779. http://dx.doi.org/10.1161/CIRCRESAHA.114.302590

Chieppa, M., M. Rescigno, A.Y. Huang, and R.N. Germain. 2006. Dynamic imaging of dendritic cell extension into the small bowel lumen in response to epithelial cell TLR engagement. *J. Exp. Med.* 203:2841–2852. http://dx.doi.org/10.1084/jem.20061884

Chodaczek, G., V. Papanna, M.A. Zal, and T. Zal. 2012. Body-barrier surveillance by epidermal γδ TCRs. *Nat. Immunol.* 13:272–282. http://dx.doi.org/10.1038/ni.2240

Choi, J.H., Y. Do, C. Cheong, H. Koh, S.B. Boscardin, Y.S. Oh, L. Bozzacco, C. Trumpfheller, C.G. Park, and R.M. Steinman. 2009. Identification of antigen-presenting dendritic cells in mouse aorta and cardiac valves. *J. Exp. Med.* 206:497–505. http://dx.doi.org/10.1084/jem.20082129

Chtanova, T., H.R. Hampton, L.A. Waterhouse, K. Wood, M. Tomura, Y. Miwa, C.R. Mackay, R. Brink, and T.G. Phan. 2014. Real-time interactive two-photon photoconversion of recirculating lymphocytes for discontinuous cell tracking in live adult mice. *J. Biophotonics.* 7:425–433. http://dx.doi.org/10.1002/jbio.201200175

Chudakov, D.M., M.V. Matz, S. Lukyanov, and K.A. Lukyanov. 2010. Fluorescent proteins and their applications in imaging living cells and tissues. *Physiol. Rev.* 90:1103–1163. http://dx.doi.org/10.1152/physrev.00038.2009

Combadière, C., S. Potteaux, J.L. Gao, B. Esposito, S. Casanova, E.J. Lee, P. Debré, A. Tedgui, P.M. Murphy, and Z. Mallat. 2003. Decreased atherosclerotic lesion formation in CX3CR1/apolipoprotein E double knockout mice. *Circulation.* 107:1009–1016. http://dx.doi.org/10.1161/01.CIR.0000057548.68243.42

Coppieters, K., M.M. Martinic, W.B. Kiosses, N. Amirian, and M. von Herrath. 2010. A novel technique for the in vivo imaging of autoimmune diabetes development in the pancreas by two-photon microscopy. *PLoS One.* 5:e15732. http://dx.doi.org/10.1371/journal.pone.0015732

Corish, P., and C. Tyler-Smith. 1999. Attenuation of green fluorescent protein half-life in mammalian cells. *Protein Eng.* 12:1035–1040. http://dx.doi.org/10.1093/protein/12.12.1035

Daley, J.M., A.A. Thomay, M.D. Connolly, J.S. Reichner, and J.E. Albina. 2008. Use of Ly6G-specific monoclonal antibody to deplete neutrophils in mice. *J. Leukoc. Biol.* 83:64–70. http://dx.doi.org/10.1189/jlb.0407247

Davey, G.M., S.N. Mueller, C. van Vliet, M. Gigowski, A. Zaid, B. Davies, F.R. Carbone, and W.R. Heath. 2013. Identification of a MHC I-restricted epitope of DsRed in C57BL/6 mice. *Mol. Immunol.* 53:450–452. http://dx.doi.org/10.1016/j.molimm.2012.10.003

Davies, P.S., A.E. Powell, J.R. Swain, and M.H. Wong. 2009. Inflammation and proliferation act together to mediate intestinal cell fusion. *PLoS One.* 4:e6530. http://dx.doi.org/10.1371/journal.pone.0006530

De Lorenzi, R., R. Gareus, S. Fengler, and M. Pasparakis. 2009. GFP-p65 knock-in mice as a tool to study NF-κB dynamics in vivo. *Genesis.* 47:323–329. http://dx.doi.org/10.1002/dvg.20468

Drechsler, M., R.T. Megens, M. van Zandvoort, C. Weber, and O. Soehnlein. 2010. Hyperlipidemia-triggered neutrophilia promotes early atherosclerosis. *Circulation*. 122:1837–1845. http://dx.doi.org/10.1161/CIRCULATIONAHA.110.961714

Drevets, D.A., B.P. Canono, and P.A. Campbell. 2015. Measurement of bacterial ingestion and killing by macrophages. *Curr. Protoc. Immunol*. 109:1–17. http://dx.doi.org/10.1002/0471142735.im1406s109

Egen, J.G., A.G. Rothfuchs, C.G. Feng, N. Winter, A. Sher, and R.N. Germain. 2008. Macrophage and T cell dynamics during the development and disintegration of mycobacterial granulomas. *Immunity.* 28:271–284. http://dx.doi.org/10.1016/j.immuni.2007.12.010

Egen, J.G., A.G. Rothfuchs, C.G. Feng, M.A. Horwitz, A. Sher, and R.N. Germain. 2011. Intravital imaging reveals limited antigen presentation and T cell effector function in mycobacterial granulomas. *Immunity.* 34:807–819. http://dx.doi.org/10.1016/j.immuni.2011.03.022

Engel, D.R., T.A. Krause, S.L. Snelgrove, S. Thiebes, M.J. Hickey, P. Boor, A.R. Kitching, and C. Kurts. 2015. CX3CR1 reduces kidney fibrosis by inhibiting local proliferation of profibrotic macrophages. *J. Immunol*. 194:1628–1638. http://dx.doi.org/10.4049/jimmunol.1402149

Eriksson, E.E., X. Xie, J. Werr, P. Thoren, and L. Lindbom. 2001a. Direct viewing of atherosclerosis in vivo: plaque invasion by leukocytes is initiated by the endothelial selectins. *FASEB J.* 15:1149–1157. http://dx.doi.org/10.1096/fj.00-0537com

Eriksson, E.E., X. Xie, J. Werr, P. Thoren, and L. Lindbom. 2001b. Importance of primary capture and L-selectin-dependent secondary capture in leukocyte accumulation in inflammation and atherosclerosis in vivo. *J. Exp. Med*. 194:205–218. http://dx.doi.org/10.1084/jem.194.2.205

Evans, T.A., D.S. Barkauskas, J.T. Myers, E.G. Hare, J.Q. You, R.M. Ransohoff, A.Y. Huang, and J. Silver. 2014. High-resolution intravital imaging reveals that blood-derived macrophages but not resident microglia facilitate secondary axonal dieback in traumatic spinal cord injury. *Exp. Neurol*. 254:109–120. http://dx.doi.org/10.1016/j.expneurol.2014.01.013

Faust, N., F. Varas, L.M. Kelly, S. Heck, and T. Graf. 2000. Insertion of enhanced green fluorescent protein into the lysozyme gene creates mice with green fluorescent granulocytes and macrophages. *Blood*. 96:719–726.

Feng, G., R.H. Mellor, M. Bernstein, C. Keller-Peck, Q.T. Nguyen, M. Wallace, J.M. Nerbonne, J.W. Lichtman, and J.R. Sanes. 2000. Imaging neuronal subsets in transgenic mice expressing multiple spectral variants of GFP. *Neuron*. 28:41–51. http://dx.doi.org/10.1016/S0896-6273(00)00084-2

Fogg, D.K., C. Sibon, C. Miled, S. Jung, P. Aucouturier, D.R. Littman, A. Cumano, and F. Geissmann. 2006. A clonogenic bone marrow progenitor specific for macrophages and dendritic cells. *Science.* 311:83–87. http://dx.doi.org/10.1126/science.1117729

Friedl, P., K. Wolf, U.H. von Andrian, and G. Harms. 2007. Biological second and third harmonic generation microscopy. *Curr. Protoc. Cell Biol*. Chapter 4:Unit 4.15. http://dx.doi.org/10.1002/0471143030.cb0415s34

Friggeri, A., Y. Yang, S. Banerjee, Y.J. Park, G. Liu, and E. Abraham. 2010. HMGB1 inhibits macrophage activity in efferocytosis through binding to the alphavbeta3-integrin. *Am. J. Physiol. Cell Physiol.* 299:C1267–C1276. http://dx.doi.org/10.1152/ajpcell.00152.2010

Fumagalli, S., F. Ortolano, and M.G. De Simoni. 2014. A close look at brain dynamics: cells and vessels seen by in vivo two-photon microscopy. *Prog. Neurobiol.* 121:36–54. http://dx.doi.org/10.1016/j.pneurobio.2014.06.005

Geissmann, F., S. Jung, and D.R. Littman. 2003. Blood monocytes consist of two principal subsets with distinct migratory properties. *Immunity.* 19:71–82. http://dx.doi.org/10.1016/S1074-7613(03)00174-2

Geissmann, F., T.O. Cameron, S. Sidobre, N. Manlongat, M. Kronenberg, M.J. Briskin, M.L. Dustin, and D.R. Littman. 2005. Intravascular immune surveillance by CXCR6+ NKT cells patrolling liver sinusoids. *PLoS Biol*. 3:e113. http://dx.doi.org/10.1371/journal.pbio.0030113

Germain, R.N., M.J. Miller, M.L. Dustin, and M.C. Nussenzweig. 2006. Dynamic imaging of the immune system: progress, pitfalls and promise. *Nat. Rev. Immunol*. 6:497–507. http://dx.doi.org/10.1038/nri1884

Germain, R.N., E.A. Robey, and M.D. Cahalan. 2012. A decade of imaging cellular motility and interaction dynamics in the immune system. *Science.* 336:1676–1681. http://dx.doi.org/10.1126/science.1221063

Gerner, M.Y., W. Kastenmuller, I. Ifrim, J. Kabat, and R.N. Germain. 2012. Histo-cytometry: a method for highly multiplex quantitative tissue imaging analysis applied to dendritic cell subset microanatomy in lymph nodes. *Immunity.* 37:364–376. http://dx.doi.org/10.1016/j.immuni.2012.07.011

Giesen, C., H.A. Wang, D. Schapiro, N. Zivanovic, A. Jacobs, B. Hattendorf, P.J. Schüffler, D. Grolimund, J.M. Buhmann, S. Brandt, et al. 2014. Highly multiplexed imaging of tumor tissues with subcellular resolution by mass cytometry. *Nat. Methods.* 11:417–422. http://dx.doi.org/10.1038/nmeth.2869

Gosselin, D., V.M. Link, C.E. Romanoski, G.J. Fonseca, D.Z. Eichenfield, N.J. Spann, J.D. Stender, H.B. Chun, H. Garner, F. Geissmann, and C.K. Glass. 2014. Environment drives selection and function of enhancers controlling tissue-specific macrophage identities. *Cell.* 159:1327–1340. http://dx.doi.org/10.1016/j.cell.2014.11.023

Grupillo, M., R. Lakomy, X. Geng, A. Styche, W.A. Rudert, M. Trucco, and Y. Fan. 2011. An improved intracellular staining protocol for efficient detection of nuclear proteins in YFP-expressing cells. *Biotechniques.* 51:417–420. http://dx.doi.org/10.2144/000113780

Gu, H., J.D. Marth, P.C. Orban, H. Mossmann, and K. Rajewsky. 1994. Deletion of a DNA polymerase beta gene segment in T cells using cell type-specific gene targeting. *Science.* 265:103–106. http://dx.doi.org/10.1126/science.8016642

Haka, A.S., S. Potteaux, H. Fraser, G.J. Randolph, and F.R. Maxfield. 2012. Quantitative analysis of monocyte subpopulations in murine atherosclerotic plaques by multiphoton microscopy. *PLoS One.* 7:e44823. http://dx.doi.org/10.1371/journal.pone.0044823

Hanna, R.N., C. Cekic, D. Sag, R. Tacke, G.D. Thomas, H. Nowyhed, E. Herrley, N. Rasquinha, S. McArdle, R. Wu, et al. 2015. Patrolling monocytes control tumor metastasis to the lung. *Science.* 350:985–990. http://dx.doi.org/10.1126/science.aac9407

Herz, J., V. Siffrin, A.E. Hauser, A.U. Brandt, T. Leuenberger, H. Radbruch, F. Zipp, and R.A. Niesner. 2010. Expanding two-photon intravital microscopy to the infrared by means of optical parametric oscillator. *Biophys. J.* 98:715–723. http://dx.doi.org/10.1016/j.bpj.2009.10.035

Herzenberg, L.A., J. Tung, W.A. Moore, L.A. Herzenberg, and D.R. Parks. 2006. Interpreting flow cytometry data: a guide for the perplexed. *Nat. Immunol.* 7:681–685. http://dx.doi.org/10.1038/ni0706-681

Horan, P.K., and S.E. Slezak. 1989. Stable cell membrane labelling. *Nature.* 340:167–168. http://dx.doi.org/10.1038/340167a0

Huo, Y., C. Weber, S.B. Forlow, M. Sperandio, J. Thatte, M. Mack, S. Jung, D.R. Littman, and K. Ley. 2001. The chemokine KC, but not monocyte chemoattractant protein-1, triggers monocyte arrest on early atherosclerotic endothelium. *J. Clin. Invest.* 108:1307–1314. http://dx.doi.org/10.1172/JCI12877

Huo, Y., A. Schober, S.B. Forlow, D.F. Smith, M.C. Hyman, S. Jung, D.R. Littman, C. Weber, and K. Ley. 2003. Circulating activated platelets exacerbate atherosclerosis in mice deficient in apolipoprotein E. *Nat. Med*. 9:61–67. http://dx.doi.org/10.1038/nm810

Iannacone, M., G. Sitia, M. Isogawa, P. Marchese, M.G. Castro, P.R. Lowenstein, F.V. Chisari, Z.M. Ruggeri, and L.G. Guidotti. 2005. Platelets mediate cytotoxic T lymphocyte-induced liver damage. *Nat. Med*. 11:1167–1169. http://dx.doi.org/10.1038/nm1317

Indra, A.K., X. Warot, J. Brocard, J.M. Bornert, J.H. Xiao, P. Chambon, and D. Metzger. 1999. Temporally-controlled site-specific mutagenesis in the basal layer of the epidermis: comparison of the recombinase activity of the tamoxifen-inducible Cre-ER(T) and Cre-ER(T2) recombinases.

Nucleic Acids Res. 27:4324–4327. http://dx.doi.org/10.1093/nar/27.22.4324

Jacquelin, S., F. Licata, K. Dorgham, P. Hermand, L. Poupel, E. Guyon, P. Deterre, D.A. Hume, C. Combadière, and A. Boissonnas. 2013. CX3CR1 reduces Ly6Chigh-monocyte motility within and release from the bone marrow after chemotherapy in mice. *Blood.* 122:674–683. http://dx.doi.org/10.1182/blood-2013-01-480749

Jenne, C.N., C.H. Wong, F.J. Zemp, B. McDonald, M.M. Rahman, P.A. Forsyth, G. McFadden, and P. Kubes. 2013. Neutrophils recruited to sites of infection protect from virus challenge by releasing neutrophil extracellular traps. *Cell Host Microbe.* 13:169–180. http://dx.doi.org/10.1016/j.chom.2013.01.005

Johnson, I.D. 2006. Practical considerations in the selection and application of fluorescent probes. In Handbook of biological confocal microscopy. James B. Pawley, editor. Springer. 353–367.

Jung, K., P. Kim, F. Leuschner, R. Gorbatov, J.K. Kim, T. Ueno, M. Nahrendorf, and S.H. Yun. 2013. Endoscopic time-lapse imaging of immune cells in infarcted mouse hearts. *Circ. Res.* 112:891–899. http://dx.doi.org/10.1161/CIRCRESAHA.111.300484

Jung, S., J. Aliberti, P. Graemmel, M.J. Sunshine, G.W. Kreutzberg, A. Sher, and D.R. Littman. 2000. Analysis of fractalkine receptor CX(3)CR1 function by targeted deletion and green fluorescent protein reporter gene insertion. *Mol. Cell. Biol.* 20:4106–4114. http://dx.doi.org/10.1128/MCB.20.11.4106-4114.2000

Kim, J.V., S.S. Kang, M.L. Dustin, and D.B. McGavern. 2009. Myelomonocytic cell recruitment causes fatal CNS vascular injury during acute viral meningitis. *Nature.* 457:191–195. http://dx.doi.org/10.1038/nature07591

Kobat, D., M.E. Durst, N. Nishimura, A.W. Wong, C.B. Schaffer, and C. Xu. 2009. Deep tissue multiphoton microscopy using longer wavelength excitation. *Opt. Express.* 17:13354–13364. http://dx.doi.org/10.1364/OE.17.013354

Kolaczkowska, E., C.N. Jenne, B.G. Surewaard, A. Thanabalasuriar, W.Y. Lee, M.J. Sanz, K. Mowen, G. Opdenakker, and P. Kubes. 2015. Molecular mechanisms of NET formation and degradation revealed by intravital imaging in the liver vasculature. *Nat. Commun.* 6:6673. http://dx.doi.org/10.1038/ncomms7673

Koltsova, E.K., Z. Garcia, G. Chodaczek, M. Landau, S. McArdle, S.R. Scott, S. von Vietinghoff, E. Galkina, Y.I. Miller, S.T. Acton, and K. Ley. 2012. Dynamic T cell-APC interactions sustain chronic inflammation in atherosclerosis. *J. Clin. Invest.* 122:3114–3126. http://dx.doi.org/10.1172/JCI61758

Koyama, K. 2002. NK1.1+ cell depletion in vivo fails to prevent protection against infection with the murine nematode parasite Trichuris muris. *Parasite Immunol.* 24:527–533. http://dx.doi.org/10.1046/j.1365-3024.2002.00497.x

Krabbe, G., A. Halle, V. Matyash, J.L. Rinnenthal, G.D. Eom, U. Bernhardt, K.R. Miller, S. Prokop, H. Kettenmann, and F.L. Heppner. 2013. Functional impairment of microglia coincides with β-amyloid deposition in mice with Alzheimer-like pathology. *PLoS One.* 8:e60921. http://dx.doi.org/10.1371/journal.pone.0060921

Kunkel, E.J., J.E. Chomas, and K. Ley. 1998. Role of primary and secondary capture for leukocyte accumulation in vivo. *Circ. Res.* 82:30–38. http://dx.doi.org/10.1161/01.RES.82.1.30

Laguna, J.C., and M. Alegret. 2012. Regulation of gene expression in atherosclerosis: insights from microarray studies in monocytes/macrophages. *Pharmacogenomics.* 13:477–495. http://dx.doi.org/10.2217/pgs.12.9

Lämmermann, T., and R.N. Germain. 2014. The multiple faces of leukocyte interstitial migration. *Semin. Immunopathol.* 36:227–251. http://dx.doi.org/10.1007/s00281-014-0418-8

Lämmermann, T., P.V. Afonso, B.R. Angermann, J.M. Wang, W. Kastenmüller, C.A. Parent, and R.N. Germain. 2013. Neutrophil swarms require LTB4 and integrins at sites of cell death in vivo. *Nature.* 498:371–375. http://dx.doi.org/10.1038/nature12175

Landsman, L., L. Bar-On, A. Zernecke, K.W. Kim, R. Krauthgamer, E. Shagdarsuren, S.A. Lira, I.L. Weissman, C. Weber, and S. Jung. 2009. CX3CR1 is required for monocyte homeostasis and atherogenesis by promoting cell survival. *Blood.* 113:963–972. http://dx.doi.org/10.1182/blood-2008-07-170787

Lassailly, F., E. Griessinger, and D. Bonnet. 2010. "Microenvironmental contaminations" induced by fluorescent lipophilic dyes used for noninvasive in vitro and in vivo cell tracking. *Blood.* 115:5347–5354. http://dx.doi.org/10.1182/blood-2009-05-224030

Last'ovicka, J., V. Budinský, R. Spísek, and J. Bartůnková. 2009. Assessment of lymphocyte proliferation: CFSE kills dividing cells and modulates expression of activation markers. *Cell. Immunol.* 256:79–85. http://dx.doi.org/10.1016/j.cellimm.2009.01.007

Lavin, Y., D. Winter, R. Blecher-Gonen, E. David, H. Keren-Shaul, M. Merad, S. Jung, and I. Amit. 2014. Tissue-resident macrophage enhancer landscapes are shaped by the local microenvironment. *Cell.* 159:1312–1326. http://dx.doi.org/10.1016/j.cell.2014.11.018

Lee, S., C. Vinegoni, P.F. Feruglio, L. Fexon, R. Gorbatov, M. Pivoravov, A. Sbarbati, M. Nahrendorf, and R. Weissleder. 2012a. Real-time in vivo imaging of the beating mouse heart at microscopic resolution. *Nat. Commun.* 3:1054. http://dx.doi.org/10.1038/ncomms2060

Lee, S., C. Vinegoni, P.F. Feruglio, and R. Weissleder. 2012b. Improved intravital microscopy via synchronization of respiration and holder stabilization. *J. Biomed. Opt.* 17:96018–1. http://dx.doi.org/10.1117/1.JBO.17.9.096018

Le Faouder, P., V. Baillif, I. Spreadbury, J.P. Motta, P. Rousset, G. Chêne, C. Guigné, F. Tercé, S. Vanner, N. Vergnolle, et al. 2013. LC-MS/MS method for rapid and concomitant quantification of pro-inflammatory and pro-resolving polyunsaturated fatty acid metabolites. *J. Chromatogr. B Analyt. Technol. Biomed. Life Sci.* 932:123–133. http://dx.doi.org/10.1016/j.jchromb.2013.06.014

Ley, K., D.C. Bullard, M.L. Arbonés, R. Bosse, D. Vestweber, T.F. Tedder, and A.L. Beaudet. 1995. Sequential contribution of L- and P-selectin to leukocyte rolling in vivo. *J. Exp. Med.* 181:669–675. http://dx.doi.org/10.1084/jem.181.2.669

Ley, K., C. Laudanna, M.I. Cybulsky, and S. Nourshargh. 2007. Getting to the site of inflammation: the leukocyte adhesion cascade updated. *Nat. Rev. Immunol.* 7:678–689. http://dx.doi.org/10.1038/nri2156

Ley, K., J. Mestas, M.K. Pospieszalska, P. Sundd, A. Groisman, and A. Zarbock. 2008. Chapter 11. Intravital microscopic investigation of leukocyte interactions with the blood vessel wall. *Methods Enzymol.* 445:255–279. http://dx.doi.org/10.1016/S0076-6879(08)03011-5

Li, C., R.K. Pastila, C. Pitsillides, J.M. Runnels, M. Puoris'haag, D. Côté, and C.P. Lin. 2010. Imaging leukocyte trafficking in vivo with two-photon-excited endogenous tryptophan fluorescence. *Opt. Express.* 18:988–999. http://dx.doi.org/10.1364/OE.18.000988

Li, J.L., C.C. Goh, J.L. Keeble, J.S. Qin, B. Roediger, R. Jain, Y. Wang, W.K. Chew, W. Weninger, and L.G. Ng. 2012a. Intravital multiphoton imaging of immune responses in the mouse ear skin. *Nat. Protoc.* 7:221–234. http://dx.doi.org/10.1038/nprot.2011.438

Li, P., R. Zhang, H. Sun, L. Chen, F. Liu, C. Yao, M. Du, and X. Jiang. 2013. PKH26 can transfer to host cells in vitro and vivo. *Stem Cells Dev.* 22:340–344. http://dx.doi.org/10.1089/scd.2012.0357

Li, W., R.G. Nava, A.C. Bribriesco, B.H. Zinselmeyer, J.H. Spahn, A.E. Gelman, A.S. Krupnick, M.J. Miller, and D. Kreisel. 2012b. Intravital 2-photon imaging of leukocyte trafficking in beating heart. *J. Clin. Invest.* 122:2499–2508. http://dx.doi.org/10.1172/JCI62970

Li, X., X. Zhao, Y. Fang, X. Jiang, T. Duong, C. Fan, C.C. Huang, and S.R. Kain. 1998. Generation of destabilized green fluorescent protein as a transcription reporter. *J. Biol. Chem.* 273:34970–34975. http://dx.doi.org/10.1074/jbc.273.52.34970

Lindquist, R.L., G. Shakhar, D. Dudziak, H. Wardemann, T. Eisenreich, M.L. Dustin, and M.C. Nussenzweig. 2004. Visualizing dendritic cell networks in vivo. *Nat. Immunol.* 5:1243–1250. http://dx.doi.org/10.1038/ni1139

Lionakis, M.S., M. Swamydas, B.G. Fischer, T.S. Plantinga, M.D. Johnson, M. Jaeger, N.M. Green, A. Masedunskas, R. Weigert, C. Mikelis, et al. 2013. CX3CR1-dependent renal macrophage survival promotes *Candida* control and host survival. *J. Clin. Invest.* 123:5035–5051. http://dx.doi.org/10.1172/JCI71307

Liu, K., G.D. Victora, T.A. Schwickert, P. Guermonprez, M.M. Meredith, K. Yao, F.F. Chu, G.J. Randolph, A.Y. Rudensky, and M. Nussenzweig. 2009. In vivo analysis of dendritic cell development and homeostasis. *Science.* 324:392–397. http://dx.doi.org/10.1126/science.1170540

Looney, M.R., E.E. Thornton, D. Sen, W.J. Lamm, R.W. Glenny, and M.F. Krummel. 2011. Stabilized imaging of immune surveillance in the mouse lung. *Nat. Methods.* 8:91–96. http://dx.doi.org/10.1038/nmeth.1543

Lyons, P.A., M. Koukoulaki, A. Hatton, K. Doggett, H.B. Woffendin, A.N. Chaudhry, and K.G. Smith. 2007. Microarray analysis of human leucocyte subsets: the advantages of positive selection and rapid purification. *BMC Genomics.* 8:64. http://dx.doi.org/10.1186/1471-2164-8-64

Majka, S.M., H.L. Miller, T. Sullivan, P.F. Erickson, R. Kong, M. Weiser-Evans, R. Nemenoff, R. Moldovan, S.A. Morandi, J.A. Davis, and D.J. Klemm. 2012. Adipose lineage specification of bone marrow-derived myeloid cells. *Adipocyte.* 1:215–229. http://dx.doi.org/10.4161/adip.21496

Marker, D.F., M.E. Tremblay, S.M. Lu, A.K. Majewska, and H.A. Gelbard. 2010. A thin-skull window technique for chronic two-photon in vivo imaging of murine microglia in models of neuroinflammation. *J. Vis. Exp.* 43:2059.

McArdle, S., S.T. Acton, K. Ley, and N. Ray. 2014. Registering sequences of in vivo microscopy images for cell tracking using dynamic programming and minimum spanning trees. In Image Processing (ICIP), 2014 IEEE International Conference. IEEE, Piscataway, NJ.

McArdle, S., G. Chodaczek, N. Ray, and K. Ley. 2015. Intravital live cell triggered imaging system reveals monocyte patrolling and macrophage migration in atherosclerotic arteries. *J. Biomed. Opt.* 20:26005. http://dx.doi.org/10.1117/1.JBO.20.2.026005

McDole, J.R., L.W. Wheeler, K.G. McDonald, B. Wang, V. Konjufca, K.A. Knoop, R.D. Newberry, and M.J. Miller. 2012. Goblet cells deliver luminal antigen to $CD103^+$ dendritic cells in the small intestine. *Nature.* 483:345–349. http://dx.doi.org/10.1038/nature10863

McNally, A.K., and J.M. Anderson. 2011. Macrophage fusion and multinucleated giant cells of inflammation. *Adv. Exp. Med. Biol.* 713:97–111. http://dx.doi.org/10.1007/978-94-007-0763-4_7

Megens, R.T., S. Reitsma, L. Prinzen, M.G. oude Egbrink, W. Engels, P.J. Leenders, E.J. Brunenberg, K.D. Reesink, B.J. Janssen, B.M. ter Haar Romeny, et al. 2010. In vivo high-resolution structural imaging of large arteries in small rodents using two-photon laser scanning microscopy. *J. Biomed. Opt.* 15:011108. http://dx.doi.org/10.1117/1.3281672

Megens, R.T., K. Kemmerich, J. Pyta, C. Weber, and O. Soehnlein. 2011. Intravital imaging of phagocyte recruitment. *Thromb. Haemost.* 105:802–810. http://dx.doi.org/10.1160/TH10-11-0735

Mempel, T.R., S.E. Henrickson, and U.H. Von Andrian. 2004. T-cell priming by dendritic cells in lymph nodes occurs in three distinct phases. *Nature.* 427:154–159. http://dx.doi.org/10.1038/nature02238

Mempel, T.R., M.J. Pittet, K. Khazaie, W. Weninger, R. Weissleder, H. von Boehmer, and U.H. von Andrian. 2006. Regulatory T cells reversibly suppress cytotoxic T cell function independent of effector differentiation. *Immunity.* 25:129–141. http://dx.doi.org/10.1016/j.immuni.2006.04.015

Miller, M.J., S.H. Wei, I. Parker, and M.D. Cahalan. 2002. Two-photon imaging of lymphocyte motility and antigen response in intact lymph node. *Science.* 296:1869–1873. http://dx.doi.org/10.1126/science.1070051

Miller, M.J., S.H. Wei, M.D. Cahalan, and I. Parker. 2003. Autonomous T cell trafficking examined in vivo with intravital two-photon microscopy. *Proc. Natl. Acad. Sci. USA.* 100:2604–2609. http://dx.doi.org/10.1073/pnas.2628040100

Milo, I., A. Sapoznikov, V. Kalchenko, O. Tal, R. Krauthgamer, N. van Rooijen, D. Dudziak, S. Jung, and G. Shakhar. 2013. Dynamic imaging reveals promiscuous crosspresentation of blood-borne antigens to naive $CD8^+$ T cells in the bone marrow. *Blood.* 122:193–208. http://dx.doi.org/10.1182/blood-2012-01-401265

Mionnet, C., V. Buatois, A. Kanda, V. Milcent, S. Fleury, D. Lair, M. Langelot, Y. Lacoeuille, E. Hessel, R. Coffman, et al. 2010. CX3CR1 is required for airway inflammation by promoting T helper cell survival and maintenance in inflamed lung. *Nat. Med.* 16:1305–1312. http://dx.doi.org/10.1038/nm.2253

Miyao, T., S. Floess, R. Setoguchi, H. Luche, H.J. Fehling, H. Waldmann, J. Huehn, and S. Hori. 2012. Plasticity of Foxp3(+) T cells reflects promiscuous Foxp3 expression in conventional T cells but not reprogramming of regulatory T cells. *Immunity.* 36:262–275. http://dx.doi.org/10.1016/j.immuni.2011.12.012

Moran, A.E., K.L. Holzapfel, Y. Xing, N.R. Cunningham, J.S. Maltzman, J. Punt, and K.A. Hogquist. 2011. T cell receptor signal strength in Treg and iNKT cell development demonstrated by a novel fluorescent reporter mouse. *J. Exp. Med.* 208:1279–1289. http://dx.doi.org/10.1084/jem.20110308

Morgan, E., R. Varro, H. Sepulveda, J.A. Ember, J. Apgar, J. Wilson, L. Lowe, R. Chen, L. Shivraj, A. Agadir, et al. 2004. Cytometric bead array: a multiplexed assay platform with applications in various areas of biology. *Clin. Immunol.* 110:252–266. http://dx.doi.org/10.1016/j.clim.2003.11.017

Norman, K.E., K.L. Moore, R.P. McEver, and K. Ley. 1995. Leukocyte rolling in vivo is mediated by P-selectin glycoprotein ligand-1. *Blood.* 86:4417–4421.

Ovchinnikov, D.A., W.J. van Zuylen, C.E. DeBats, K.A. Alexander, S. Kellie, and D.A. Hume. 2008. Expression of Gal4-dependent transgenes in cells of the mononuclear phagocyte system labeled with enhanced cyan fluorescent protein using Csf1r-Gal4VP16/UAS-ECFP double-transgenic mice. *J. Leukoc. Biol.* 83:430–433. http://dx.doi.org/10.1189/jlb.0807585

Parish, C.R. 1999. Fluorescent dyes for lymphocyte migration and proliferation studies. *Immunol. Cell Biol.* 77:499–508. http://dx.doi.org/10.1046/j.1440-1711.1999.00877.x

Patterson, G.H., and J. Lippincott-Schwartz. 2002. A photoactivatable GFP for selective photolabeling of proteins and cells. *Science.* 297:1873–1877. http://dx.doi.org/10.1126/science.1074952

Pawelczyk, E., E.K. Jordan, A. Balakumaran, A. Chaudhry, N. Gormley, M. Smith, B.K. Lewis, R. Childs, P.G. Robey, and J.A. Frank. 2009. In vivo transfer of intracellular labels from locally implanted bone marrow stromal cells to resident tissue macrophages. *PLoS One.* 4:e6712. http://dx.doi.org/10.1371/journal.pone.0006712

Peters, N.C., J.G. Egen, N. Secundino, A. Debrabant, N. Kimblin, S. Kamhawi, P. Lawyer, M.P. Fay, R.N. Germain, and D. Sacks. 2008. In vivo imaging reveals an essential role for neutrophils in leishmaniasis transmitted by sand flies. *Science.* 321:970–974. http://dx.doi.org/10.1126/science.1159194

Phillipson, M., B. Heit, P. Colarusso, L. Liu, C.M. Ballantyne, and P. Kubes. 2006. Intraluminal crawling of neutrophils to emigration sites: a molecularly distinct process from adhesion in the recruitment cascade. *J. Exp. Med.* 203:2569–2575. http://dx.doi.org/10.1084/jem.20060925

Poon, R.Y., B.M. Ohlsson-Wilhelm, C.B. Bagwell, and K.A. Muirhead. 2000. Use of PKH membrane intercalating dyes to monitor cell trafficking and function. In In Living Color. Rochelle A. Diamond, and Susan Demaggio, editors. Springer. 302–352.

Potteaux, S., E.L. Gautier, S.B. Hutchison, N. van Rooijen, D.J. Rader, M.J. Thomas, M.G. Sorci-Thomas, and G.J. Randolph. 2011. Suppressed monocyte recruitment drives macrophage removal from atherosclerotic plaques of *Apoe*$^{-/-}$ mice during disease regression. *J. Clin. Invest.* 121:2025–2036. http://dx.doi.org/10.1172/JCI43802

Potter, S.M., C.-M. Wang, P.A. Garrity, and S.E. Fraser. 1996. Intravital imaging of green fluorescent protein using two-photon laser-scanning microscopy. *Gene.* 173:25–31. http://dx.doi.org/10.1016/0378-1119(95)00681-8

Progatzky, F., M.J. Dallman, and C. Lo Celso. 2013. From seeing to believing: labelling strategies for in vivo cell-tracking experiments. *Interface Focus.* 3:20130001. http://dx.doi.org/10.1098/rsfs.2013.0001

Rademakers, T., K. Douma, T.M. Hackeng, M.J. Post, J.C. Sluimer, M.J. Daemen, E.A. Biessen, S. Heeneman, and M.A. van Zandvoort. 2013. Plaque-associated vasa vasorum in aged apolipoprotein E-deficient mice exhibit proatherogenic functional features in vivo. *Arterioscler. Thromb. Vasc. Biol.* 33:249–256. http://dx.doi.org/10.1161/ATVBAHA.112.300087

Ray, N., S. McArdle, K. Lay, and S. Acton. 2015. MISTICA: minimum spanning tree-based coarse image alignment for microscopy image sequences. *IEEE J. Biomed. Health Inform.*:1. http://dx.doi.org/10.1109/JBHI.2015.2480712

Sacchetti, A., T. El Sewedy, A.F. Nasr, and S. Alberti. 2001. Efficient GFP mutations profoundly affect mRNA transcription and translation rates. *FEBS Lett.* 492:151–155. http://dx.doi.org/10.1016/S0014-5793(01)02246-3

Saederup, N., A.E. Cardona, K. Croft, M. Mizutani, A.C. Cotleur, C.L. Tsou, R.M. Ransohoff, and I.F. Charo. 2010. Selective chemokine receptor usage by central nervous system myeloid cells in CCR2-red fluorescent protein knock-in mice. *PLoS One.* 5:e13693. http://dx.doi.org/10.1371/journal.pone.0013693

Sasmono, R.T., D. Oceandy, J.W. Pollard, W. Tong, P. Pavli, B.J. Wainwright, M.C. Ostrowski, S.R. Himes, and D.A. Hume. 2003. A macrophage colony-stimulating factor receptor-green fluorescent protein transgene is expressed throughout the mononuclear phagocyte system of the mouse. *Blood.* 101:1155–1163. http://dx.doi.org/10.1182/blood-2002-02-0569

Sauter, K.A., C. Pridans, A. Sehgal, C.C. Bain, C. Scott, L. Moffat, R. Rojo, B.M. Stutchfield, C.L. Davies, D.S. Donaldson, et al. 2014. The MacBlue binary transgene (csf1r-gal4VP16/UAS-ECFP) provides a novel marker for visualisation of subsets of monocytes, macrophages and dendritic cells and responsiveness to CSF1 administration. *PLoS One.* 9:e105429. http://dx.doi.org/10.1371/journal.pone.0105429

Schindler, S.E., J.G. McCall, P. Yan, K.L. Hyrc, M. Li, C.L. Tucker, J.M. Lee, M.R. Bruchas, and M.I. Diamond. 2015. Photo-activatable Cre recombinase regulates gene expression in vivo. *Sci. Rep.* 5:13627. http://dx.doi.org/10.1038/srep13627

Schulz, O., M. Ugur, M. Friedrichsen, K. Radulovic, J.H. Niess, S. Jalkanen, A. Krueger, and O. Pabst. 2014. Hypertrophy of infected Peyer's patches arises from global, interferon-receptor, and CD69-independent shut-down of lymphocyte egress. *Mucosal Immunol.* 7:892–904.

Shaked, I., R.N. Hanna, H. Shaked, G. Chodaczek, H.N. Nowyhed, G. Tweet, R. Tacke, A.B. Basat, Z. Mikulski, S. Togher, et al. 2015. Transcription factor Nr4a1 couples sympathetic and inflammatory cues in CNS-recruited macrophages to limit neuroinflammation. *Nat. Immunol.* 16:1228–1234. http://dx.doi.org/10.1038/ni.3321

Shaner, N.C., R.E. Campbell, P.A. Steinbach, B.N. Giepmans, A.E. Palmer, and R.Y. Tsien. 2004. Improved monomeric red, orange and yellow fluorescent proteins derived from Discosoma sp. red fluorescent protein. *Nat. Biotechnol.* 22:1567–1572. http://dx.doi.org/10.1038/nbt1037

Shaner, N.C., P.A. Steinbach, and R.Y. Tsien. 2005. A guide to choosing fluorescent proteins. *Nat. Methods.* 2:905–909. http://dx.doi.org/10.1038/nmeth819

Smith, M.L., D.S. Long, E.R. Damiano, and K. Ley. 2003. Near-wall micro-PIV reveals a hydrodynamically relevant endothelial surface layer in venules in vivo. *Biophys. J.* 85:637–645. http://dx.doi.org/10.1016/S0006-3495(03)74507-X

Snippert, H.J., L.G. van der Flier, T. Sato, J.H. van Es, M. van den Born, C. Kroon-Veenboer, N. Barker, A.M. Klein, J. van Rheenen, B.D. Simons, and H. Clevers. 2010. Intestinal crypt homeostasis results from neutral competition between symmetrically dividing Lgr5 stem cells. *Cell.* 143:134–144. http://dx.doi.org/10.1016/j.cell.2010.09.016

Soos, T.J., T.N. Sims, L. Barisoni, K. Lin, D.R. Littman, M.L. Dustin, and P.J. Nelson. 2006. CX3CR1+ interstitial dendritic cells form a contiguous network throughout the entire kidney. *Kidney Int.* 70:591–596. http://dx.doi.org/10.1038/sj.ki.5001567

Soriano, P. 1999. Generalized lacZ expression with the ROSA26 Cre reporter strain. *Nat. Genet.* 21:70–71. http://dx.doi.org/10.1038/5007

Soulet, D., A. Paré, J. Coste, and S. Lacroix. 2013. Automated filtering of intrinsic movement artifacts during two-photon intravital microscopy. *PLoS One.* 8:e53942. http://dx.doi.org/10.1371/journal.pone.0053942

Stark, K., A. Eckart, S. Haidari, A. Tirniceriu, M. Lorenz, M.L. von Brühl, F. Gärtner, A.G. Khandoga, K.R. Legate, R. Pless, et al. 2013. Capillary and arteriolar pericytes attract innate leukocytes exiting through venules and 'instruct' them with pattern-recognition and motility programs. *Nat. Immunol.* 14:41–51. http://dx.doi.org/10.1038/ni.2477

Stoll, S., J. Delon, T.M. Brotz, and R.N. Germain. 2002. Dynamic imaging of T cell-dendritic cell interactions in lymph nodes. *Science.* 296:1873–1876. http://dx.doi.org/10.1126/science.1071065

Sumen, C., T.R. Mempel, I.B. Mazo, and U.H. von Andrian. 2004. Intravital microscopy: visualizing immunity in context. *Immunity.* 21:315–329. http://dx.doi.org/10.1016/j.immuni.2004.08.006

Sundd, P., and K. Ley. 2013. Quantitative dynamic footprinting microscopy. *Immunol. Cell Biol.* 91:311–320. http://dx.doi.org/10.1038/icb.2012.84

Susaki, E.A., K. Tainaka, D. Perrin, H. Yukinaga, A. Kuno, and H.R. Ueda. 2015. Advanced CUBIC protocols for whole-brain and whole-body clearing and imaging. *Nat. Protoc.* 10:1709–1727. http://dx.doi.org/10.1038/nprot.2015.085

Sutton, E.J., T.D. Henning, B.J. Pichler, C. Bremer, and H.E. Daldrup-Link. 2008. Cell tracking with optical imaging. *Eur. Radiol.* 18:2021–2032. http://dx.doi.org/10.1007/s00330-008-0984-z

Swirski, F.K., M. Nahrendorf, M. Etzrodt, M. Wildgruber, V. Cortez-Retamozo, P. Panizzi, J.L. Figueiredo, R.H. Kohler, A. Chudnovskiy, P. Waterman, et al. 2009. Identification of splenic reservoir monocytes and their deployment to inflammatory sites. *Science.* 325:612–616. http://dx.doi.org/10.1126/science.1175202

Tacke, F., D. Alvarez, T.J. Kaplan, C. Jakubzick, R. Spanbroek, J. Llodra, A. Garin, J. Liu, M. Mack, N. van Rooijen, et al. 2007. Monocyte subsets differentially employ CCR2, CCR5, and CX3CR1 to accumulate within atherosclerotic plaques. *J. Clin. Invest.* 117:185–194. http://dx.doi.org/10.1172/JCI28549

Tomer, R., L. Ye, B. Hsueh, and K. Deisseroth. 2014. Advanced CLARITY for rapid and high-resolution imaging of intact tissues. *Nat. Protoc.* 9:1682–1697. http://dx.doi.org/10.1038/nprot.2014.123

Tomura, M., N. Yoshida, J. Tanaka, S. Karasawa, Y. Miwa, A. Miyawaki, and O. Kanagawa. 2008. Monitoring cellular movement in vivo with photoconvertible fluorescence protein "Kaede" transgenic mice. *Proc. Natl. Acad. Sci. USA.* 105:10871–10876. http://dx.doi.org/10.1073/pnas.0802278105

Tomura, M., A. Hata, S. Matsuoka, F.H. Shand, Y. Nakanishi, R. Ikebuchi, S. Ueha, H. Tsutsui, K. Inaba, K. Matsushima, et al. 2014. Tracking and quantification of dendritic cell migration and antigen trafficking between the skin and lymph nodes. *Sci. Rep.* 4:6030. http://dx.doi.org/10.1038/srep06030

Vadakkan, T.J., J.C. Culver, L. Gao, T. Anhut, and M.E. Dickinson. 2009. Peak multiphoton excitation of mCherry using an optical parametric oscillator (OPO). *J. Fluoresc.* 19:1103–1109. http://dx.doi.org/10.1007/s10895-009-0510-y

van Zandvoort, M., W. Engels, K. Douma, L. Beckers, M. Oude Egbrink, M. Daemen, and D.W. Slaaf. 2004. Two-photon microscopy for imaging of the (atherosclerotic) vascular wall: a proof of concept study. *J. Vasc. Res.* 41:54–63. http://dx.doi.org/10.1159/000076246

Varol, C., A. Vallon-Eberhard, E. Elinav, T. Aychek, Y. Shapira, H. Luche, H.J. Fehling, W.D. Hardt, G. Shakhar, and S. Jung. 2009. Intestinal lamina propria dendritic cell subsets have different origin and functions. *Immunity.* 31:502–512. http://dx.doi.org/10.1016/j.immuni.2009.06.025

Victora, G.D., T.A. Schwickert, D.R. Fooksman, A.O. Kamphorst, M. Meyer-Hermann, M.L. Dustin, and M.C. Nussenzweig. 2010. Germinal center dynamics revealed by multiphoton microscopy with a photoactivatable fluorescent reporter. *Cell.* 143:592–605. http://dx.doi.org/10.1016/j.cell.2010.10.032

Vinegoni, C., S. Lee, R. Gorbatov, and R. Weissleder. 2012. Motion compensation using a suctioning stabilizer for intravital microscopy. *Intravital.* 1:115–121. http://dx.doi.org/10.4161/intv.23017

Vinegoni, C., S. Lee, P.F. Feruglio, P. Marzola, M. Nahrendorf, and R. Weissleder. 2013. Sequential average segmented microscopy for high signal-to-noise ratio motion-artifact-free in vivo heart imaging. *Biomed. Opt. Express.* 4:2095–2106. http://dx.doi.org/10.1364/BOE.4.002095

Vinegoni, C., S. Lee, P.F. Feruglio, and R. Weissleder. 2014. Advanced Motion Compensation Methods for Intravital Optical Microscopy. *IEEE J. Sel. Top. Quantum Electron.* 20:1–9. http://dx.doi.org/10.1109/JSTQE.2013.2279314

Wagner, R.I. 1839. Erläuterungstafeln zur Physiologie und Entwickelungsgeschichte mit vorzüglicher Rücksicht auf feine Lehrbücher über Physiologie und vergleichende Anatomie.

Wang, X., H. Sumida, and J.G. Cyster. 2014. GPR18 is required for a normal CD8αα intestinal intraepithelial lymphocyte compartment. *J. Exp. Med.* 211:2351–2359. http://dx.doi.org/10.1084/jem.20140646

Wyckoff, J.B., Y. Wang, E.Y. Lin, J.F. Li, S. Goswami, E.R. Stanley, J.E. Segall, J.W. Pollard, and J. Condeelis. 2007. Direct visualization of macrophage-assisted tumor cell intravasation in mammary tumors. *Cancer Res.* 67:2649–2656. http://dx.doi.org/10.1158/0008-5472.CAN-06-1823

Xu, S., Y. Huang, Y. Xie, T. Lan, K. Le, J. Chen, S. Chen, S. Gao, X. Xu, X. Shen, et al. 2010. Evaluation of foam cell formation in cultured macrophages: an improved method with Oil Red O staining and DiI-oxLDL uptake. *Cytotechnology.* 62:473–481. http://dx.doi.org/10.1007/s10616-010-9290-0

Yang, X.W., and S. Gong. 2005. An overview on the generation of BAC transgenic mice for neuroscience research. Current protocols in neuroscience. Chapter 5:Unit 5.

Yokomizo, T., T. Yamada-Inagawa, A.D. Yzaguirre, M.J. Chen, N.A. Speck, and E. Dzierzak. 2012. Whole-mount three-dimensional imaging of internally localized immunostained cells within mouse embryos. *Nat. Protoc.* 7:421–431. http://dx.doi.org/10.1038/nprot.2011.441

Yona, S., K.W. Kim, Y. Wolf, A. Mildner, D. Varol, M. Breker, D. Strauss-Ayali, S. Viukov, M. Guilliams, A. Misharin, et al. 2013. Fate mapping reveals origins and dynamics of monocytes and tissue macrophages under homeostasis. *Immunity.* 38:79–91. http://dx.doi.org/10.1016/j.immuni.2012.12.001

Yu, W., J.C. Braz, A.M. Dutton, P. Prusakov, and M. Rekhter. 2007. In vivo imaging of atherosclerotic plaques in apolipoprotein E deficient mice using nonlinear microscopy. *J. Biomed. Opt.* 12:054008. http://dx.doi.org/10.1117/1.2800337

Zal, T., and G. Chodaczek. 2010. Intravital imaging of anti-tumor immune response and the tumor microenvironment. *Semin. Immunopathol.* 32:305–317. http://dx.doi.org/10.1007/s00281-010-0217-9

Zinselmeyer, B.H., J.N. Lynch, X. Zhang, T. Aoshi, and M.J. Miller. 2008. Video-rate two-photon imaging of mouse footpad - a promising model for studying leukocyte recruitment dynamics during inflammation. *Inflamm. Res.* 57:93–96. http://dx.doi.org/10.1007/s00011-007-7195-y

Zinselmeyer, B.H., J. Dempster, D.L. Wokosin, J.J. Cannon, R. Pless, I. Parker, and M.J. Miller. 2009. Chapter 16. Two-photon microscopy and multidimensional analysis of cell dynamics. *Methods Enzymol.* 461:349–378. http://dx.doi.org/10.1016/S0076-6879(09)05416-0

Zoumi, A., A. Yeh, and B.J. Tromberg. 2002. Imaging cells and extracellular matrix in vivo by using second-harmonic generation and two-photon excited fluorescence. *Proc. Natl. Acad. Sci. USA.* 99:11014–11019. http://dx.doi.org/10.1073/pnas.172368799